

43 where *in situ* data collection is more difficult, and interest in them is growing within the environmental policy
44 communities. We review these developments, identify new opportunities and scientific priorities, and identify
45 that the formation of an international advisory group could accelerate policy relevant advancements within
46 both the ocean carbon and satellite communities. Some barriers to understanding exist but these should not
47 stop the exploitation and the full visibility of satellite observations to policy makers and users, so these
48 observations can fulfil their full potential and recognition for supporting society.

49

50 **1. Introduction**

51 The latest assessment by the Intergovernmental Panel on Climate Change (IPCC) on the state of our climate
52 identified that warming of 1.5°C appears unavoidable (IPCC, 2022) and that rapid emissions reductions are
53 urgently needed to reduce further warming and stabilise climate. These recommendations are guided by
54 annual assessments of the carbon budget (e.g. by the Global Carbon Project, GCP) which attempt to
55 quantify annual emissions (fossil fuel, cement production, land use change), their redistribution within the
56 atmosphere and their uptake by the land biosphere and the ocean (e.g. Friedlingstein *et al.*, 2019, 2020,
57 2022). The relatively well-mixed nature of the atmosphere allows the quantification of the long-term CO₂
58 accumulation using a small number of observing stations (e.g. Keeling, 1978). Observation-based estimates
59 of the annual ocean carbon uptake (sink) have now become a key component within these assessments,
60 complementing the ocean model-based estimates. In contrast, the land sink continues to be estimated via
61 models (Friedlingstein *et al.*, 2022) due to its highly heterogeneous nature. Thus, ocean and atmosphere
62 observations form the key observational pillars and constraints within these annual carbon budget
63 assessments, with their uncertainties directly impacting the closure of the total budget. The policy relevance
64 of these annual carbon assessments cannot be underestimated; they provide information about the impact of
65 mitigation policies and they also enable updates on the so called “remaining carbon budget”, which identifies
66 how much CO₂ can be emitted in the coming decades without overshooting specific climate targets (e.g. as
67 determined using models within IPCC, 2022 and Friedlingstein *et al.*, 2022). Thus, efforts to increase
68 understanding of, as well as improve the quantification of the ocean carbon sink, will strengthen its constraint
69 on the remaining components of the budget within annual assessments, and increase the strength of any
70 resulting policy guidance.

71

72 Models and the analyses of ocean interior observations show that more than a quarter of the total
73 anthropogenic emissions have been taken up by the ocean (Sabine *et al.*, 2004; Gruber *et al.*, 2019b) with
74 the proportion absorbed remaining near constant over the last five decades (Friedlingstein *et al.*, 2022;
75 Gruber *et al.*, 2023). This uptake occurs predominantly through gas exchange across the atmosphere-ocean
76 interface and penetrates into the subsurface layers, changing the marine carbonate chemistry. The net effect
77 is often called “Ocean Acidification” and is detrimental to marine life and the ocean’s ability to function as a
78 carbon sink. This ocean acidification encompasses the anthropogenic CO₂ driven increase in acidity ([H⁺],
79 decreasing in pH), the increase in the concentration of dissolved CO₂, the decrease in the concentration of
80 the carbonate ion and the resulting decrease in the saturation state of seawater with regard to solid forms of
81 calcium carbonate such as aragonite and calcite (e.g. Feely *et al.*, 2009). Ocean acidification is decreasing
82 the ocean’s capacity to absorb further CO₂ (Orr *et al.*, 2005) and its impact on marine organisms and
83 ecosystems varies substantially across taxa and systems, but tends to be especially detrimental for
84 calcifying organisms, including those with significant economic or ecological importance such as corals,

85 mussels, and pelagic calcifiers (e.g. Dixon *et al.*, 2022; Doney *et al.* 2020). The changes induced by ocean
86 acidification percolate up entire food webs, populations and ecosystems, threatening essential marine
87 ecosystem services (Sunday *et al.*, 2017; Fabry *et al.*, 2019) such as coastal or flood protection and fisheries
88 (e.g. Doney *et al.*, 2020) and degrading their related socio-economical values.

89
90 Historically, most knowledge about global ocean carbon was derived from models (Gruber *et al.*, 2023) but
91 since the 1990s ocean observations are providing an increasing number of constraints. Within this *in situ*
92 observations are critical, but given the ocean's size and its often inhospitable nature, their coverage remains
93 limited. The unique capability of space-based observations for providing large spatial scale (figure 1a), and
94 increasingly regional-scale, observations means that they are now heavily used alongside *in situ*
95 observations. Beyond the differences in spatial coverage, this combination is needed as some key properties
96 cannot be observed from space but can be *in situ* (e.g. gaseous CO₂ within the ocean), whilst some
97 observations require specialist *in situ* capability not routinely available, but which is routinely deployed in
98 space (e.g. near-infrared sensed temperature at 1 mm depth, or microwave evaluation of ice coverage). Just
99 as *in situ* instruments require regular laboratory calibrations, satellite instruments require regular monitoring
100 and calibration via *in situ* data. Consequently, the ability to use satellite observations relies upon *in situ* data
101 campaigns, and global and regional observation-based assessments of ocean carbon rely heavily upon the
102 integration of satellite observations with extensive *in situ* data and model re-analyses (Shutler *et al.*, 2020).

103
104 Clearly the only way to slow the rate of ocean acidification is to drastically reduce the rate of the human-
105 made emissions of CO₂, in order to, at least stabilize the atmospheric CO₂ concentration, and satellite and *in*
106 *situ* observation-based ocean carbon assessments will be critical to identify any stabilisation. Even when
107 stabilisation occurs, we will need mitigation and adaption strategies and satellite observations are well
108 placed to support these. Similarly, a plethora of outstanding, and critical, science questions that carbon-cycle
109 communities are now focussing on, such as identifying the strength and role of the Southern Ocean carbon
110 sink (e.g. Gruber *et al.*, 2019), or the importance of ocean biology in modulating carbon exchange and how
111 this will change (e.g. Arico *et al.*, 2020) will all require the use of satellite observations.

112
113 This paper, supported with new primary data, first reviews how and why satellite observations are critical to
114 ocean carbon science and assessments. It then identifies new scientific opportunities and key areas where
115 satellite observations will provide greatest benefit to the carbon community, and identifies how to strengthen
116 the important link between these satellite observation-based approaches and potential end users, a link that
117 is currently weak. This includes mapping how the satellite capabilities could be used to support mitigation
118 and adaption at regional and international levels. This map has been co-designed with early adopters whose
119 communities are already grappling with the decreasing pH of their seas. This paper forms part of a special
120 issue and accompanies the work of Brewin *et al.*, (2023) which identifies the capabilities for studying
121 inorganic and organic ocean carbon from space, and a large range of scientific needs. This paper expands
122 upon this by focussing solely on the ocean carbon sink and ocean acidification, identifying scientific and
123 policy priorities and opportunities for quantifying surface water inorganic carbon.

124

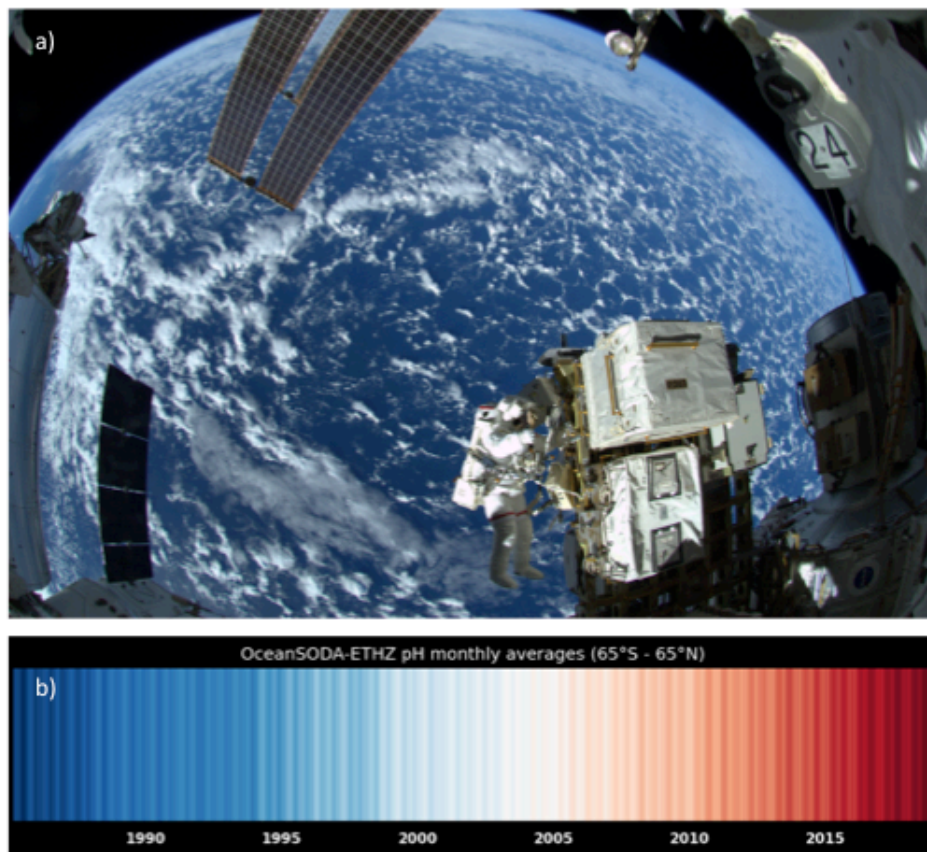


Figure 1: Satellite Earth observations are already used extensively to study ocean health and increasingly ocean acidification. a) This view of the Pacific Ocean from the largest satellite ever built, the International Space Station, illustrates the synoptic-scale view uniquely provided by satellite observations – everything in this view is the Pacific Ocean (credit, European Space Agency). This platform has hosted >30 different experimental satellite sensors which have yet to be explored by the ocean carbon community; b) The ‘pH stripe’ highlighting the long-term change in ocean pH since the 1980s, as determined using satellite observation-based data illustrates how satellite observations can help highlight the impact that carbon emissions are having on ocean health (generated using data from Gregor and Gruber, 2021).

125

126 **2. Satellite data are extensively used for ocean carbon assessments**

127 The relationships between the different carbonate system parameters are fundamentally driven by
 128 thermodynamics. Salinity directly affects the coefficients of the carbonate system equations (Land *et al.*,
 129 2015) and covaries with alkalinity across the globe (Millero *et al.*, 1998; Lee *et al.*, 2006). Temperature is a
 130 strong controller of CO₂ solubility (Woolf *et al.*, 2016); so temperature and salinity are highly related to
 131 changes in dissolved inorganic carbon (e.g. Bakker *et al.*, 1999). Hence, temperature and salinity are
 132 important diagnostic variables and are needed to assess the surface water carbonate system (Dickson *et al.*,
 133 2007). This has led to satellite temperature data now routinely being used to identify the causes of wider
 134 spatial scale variability in the surface carbonate system (e.g. Lefevre *et al.*, 2021; Olivier *et al.*, 2022). The
 135 relatively recent capability for satellite salinity observations has unlocked the ability for space-based
 136 carbonate system monitoring (Land *et al.*, 2015; Salisbury *et al.*, 2015) of surface waters via empirically
 137 derived salinity-alkalinity relationships. Early work demonstrated its credibility enabling the first observations
 138 of synoptic scale alkalinity in the Atlantic (Fine *et al.*, 2016), and alkalinity and dissolved carbon temporal

139 mixing in the Amazon plume (Land *et al.*, 2019). The use of machine learning has produced observation-
140 driven decadal-scale assessments of a single carbon parameter (partial pressure of CO₂, e.g. Watson *et al.*,
141 2020; Chau *et al.*, 2022; Friedlingstein *et al.*, 2021; figure 2) and even the complete carbonate system
142 (Gregor and Gruber, 2021; figure 2) through combining the satellite observations with large *in situ* databases
143 (Global Ocean Data Analysis Project, GLODAP, Lauvset *et al.*, (2021) or the Surface Ocean CO₂ Atlas,
144 SOCAT, Bakker *et al.*, 2016). Such methods extensively rely on satellite temperature, wind speed, sea
145 surface height and ocean colour, in conjunction with *in situ* re-analyses or climatologies, to identify the
146 underlying processes controlling in-water concentrations. For ocean sink assessments, the direction of
147 exchange with the atmosphere is determined by the CO₂ concentration above and below the atmosphere-
148 ocean interface, whereas the turbulent exchange itself is primarily water-side controlled so it is routinely
149 characterised using sea surface temperature and wind speed data (e.g. Ho *et al.*, 2016). An array of
150 methods combine elements of all of these satellite approaches to determine the CO₂ concentrations along
151 with satellite observed ice coverage and re-analysis data (e.g. for atmospheric conditions) to calculate
152 atmosphere-ocean CO₂ exchange and the net carbon sink (e.g. the eight methods presented within
153 Friedlingstein *et al.* (2021) and its annual updates used to guide policy; the six methods within Fay *et al.*,
154 2021). This use of satellite remote sensing has enabled the ocean carbon community to reconstruct multi-
155 decadal ocean carbon assessments. These efforts have been encouraged and supported by international
156 carbon observing strategies (e.g. CEOS, 2014; GOA-ON 2019; Tilbrook *et al.*, 2019) and individual scientific
157 community efforts (e.g. the international Surface Ocean and Lower Atmosphere Study, SOLAS). Collectively
158 this exploitation means that satellite observations have become critical for assessing marine carbon and the
159 impact that carbon absorption is having on ocean ecosystems and health (Shutler *et al.*, 2020; Arico *et al.*,
160 2021). They are therefore being used to guide policy and have now been identified as important for
161 supporting delivery of the UN Ocean Decade outcomes (Dobson *et al.*, in-press; Arico *et al.*, 2021). Despite
162 these advances in understanding and capability, the critical importance of satellite observations for such
163 assessments, along with the fragile nature of any underlying *in situ* networks (e.g. SOCAT) on which they
164 also rely, is often opaque to, or overlooked by, policy makers. Clearly, the routine integration of all forms of
165 observations, combining satellite and *in situ* observations from ships, moorings, and robotic platforms is now
166 possible. And sustained funding and international prioritization mechanisms would enable an integrated
167 global carbon observing network (Shutler *et al.*, 2020) to better inform and support policy decisions and
168 outcomes.
169

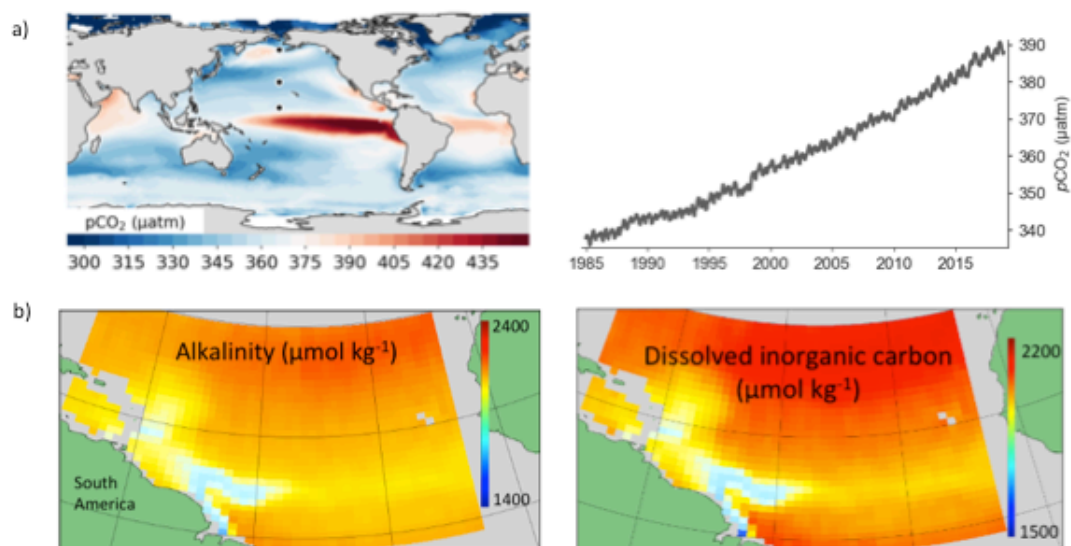


Figure 2: Recent advances in satellite observation-based data for studying the surface water marine carbonate system. a) Global assessments of the amount of gaseous CO₂ (pCO₂) can be mapped using satellite observations in conjunction with *in situ* databases to provide decadal-scale monthly data inputs to annual carbon assessments (i.e. Friedlingstein *et al.*, 2021) (data from Gregor and Gruber, 2021); b) Regional assessments using satellite observation-based methods can quantify alkalinity and dissolved carbon flowing from the Amazon into the Atlantic (data from Land *et al.*, 2019).

170

171 3. Achievable advances needed within the next 2 to 5 years

172 The following sections identify how remote sensing advances in ocean carbon research can help further
 173 constrain the global carbon budget and benefit the wider carbon community increasing the ability to guide,
 174 advise and manage mitigation, adaptation and conservation efforts.

175

176 3.1 Scientific advances in understanding or capability

177 Six areas of scientific importance where satellite observations can play a critical role are discussed in the
 178 following sections. Satellite approaches hold the potential for: reducing major sources of uncertainties in
 179 global ocean carbon assessments (section 3.1.1); addressing inconsistencies between observed and re-
 180 analysis assessments of upper ocean mixing (section 3.1.2); quantifying the variability and trends in land to
 181 ocean carbon exchange (section 3.1.3); resolving meso-scale features and variability for supporting regional
 182 and local-scale assessments of ocean acidification (section 3.1.4); identifying those regions and times where
 183 compound events are occurring (section 3.1.5), and for understanding the role of biology in the evolution of
 184 the long-term ocean carbon sink (section 3.1.6).

185

186 3.1.1 Exploring the air-sea interface

187 Despite the focus on global-scale assessments, the actual exchange of CO₂ occurs across a sub-millimetre
 188 depth of the mass boundary layer where the atmosphere and ocean interact. Small gradients in
 189 concentration either side of this interface are considered significant when scaled globally (Bellenger *et al.*,
 190 2023; Goddijn-murphy *et al.*, 2015; Dong *et al.*, 2022; Watson *et al.*, 2020; Woolf *et al.*, 2016; Shutler *et al.*,
 191 2020), and the water-side control of CO₂ exchange implies that the water-side gradients are particularly
 192 important. Improved understanding of the impact of near-surface temperature gradients (Woolf *et al.*, 2016)

193 has helped to advance satellite observation-based assessments of the ocean carbon sink (e.g. Dong *et al.*,
194 2022; Shutler *et al.*, 2020; Woolf *et al.*, 2019; Watson *et al.*, 2020;), but debate continues over their
195 significance as field evidence of the impact of these gradients is lacking (Friedlingstein *et al.*, 2022).
196 Microwave penetration depth in water is within the mass boundary layer and therefore microwave observed
197 temperatures can be considered a sub-skin temperature (Minnett *et al.*, 2019), whereas infra-red
198 observations are close to the atmosphere-ocean interface. Coincident ship-mounted remotely sensed infra-
199 red and passive microwave temperature observations could therefore enable the temperature across the
200 mass boundary layer to be experimentally evaluated in the field; measurements that could then constrain a
201 high-resolution turbulence model (e.g. as used within Merchant *et al.*, 2019) or be compared with boundary
202 layer imaging from advanced air-sea interaction facilities (e.g. Nagal *et al.*, 2015) to provide the missing
203 evidence sought by the wider carbon community. Similarly, passive microwave satellite salinity retrievals
204 originating from within the mass boundary layer could help further refine our understanding of near-surface
205 salinity gradients (as haline gradients can also occur; e.g. Woolf *et al.*, 2016).

206
207 The parameterisation and understanding of the atmosphere-ocean exchange of gases is considered the
208 major source of uncertainty within global scale ocean carbon sink assessments (e.g., Woolf *et al.*, 2019).
209 Passive microwave measurements across multiple wavelengths contain the signature of key processes
210 controlling this surface exchange and offer a unique and largely untapped resource for direct observations of
211 multiple exchange processes, which could reduce the reliance on wind-speed based proxies of air-sea gas
212 exchange (Shutler *et al.*, 2020). Whilst future passive microwave satellite concepts will provide significant
213 opportunities for simultaneously studying multiple ocean-atmosphere processes to enable more advanced
214 understanding of these interactions (e.g., Ciani *et al.*, 2019; Gentemann *et al.*, 2020). It may also be
215 possible to observe or parameterise alkalinity directly from passive microwave emissivity data, in contrast to
216 current methods (e.g., Land *et al.*, 2019) which rely on the emissivity derived salinity to then derive alkalinity.
217 Such efforts could focus on long-standing microwave sensors designed for salinity (e.g., the soil moisture
218 and ocean salinity satellite mission, SMOS) through exploiting large alkalinity datasets (e.g., Lauvset *et al.*,
219 2021) and regions of high data densities like the Atlantic. Whereas the potential and advantages of using
220 satellite backscatter to parameterize gas exchange has been previously highlighted (Shutler *et al.*, 2020) but
221 no new advances have so far appeared despite a plethora of suitable satellite sensors already in orbit, and
222 the development of ship mounted synthetic aperture radar instruments means that radar focused gas
223 exchange experiments are now feasible.

224

225 **3.1.2 Connecting the interface with the sub-surface and upper ocean dynamics and mixing**

226 The conditions below the surface can enhance or diminish the surface carbon absorption and alter the
227 carbonate system state, and surface observed conditions can provide insights into the processes or
228 conditions occurring at depth. Dependent upon the sensing technology the relevant depth of satellite
229 observations can range from sub-millimeter (e.g. thermal infrared) down to tens of meters (e.g., ocean colour
230 in an oligotrophic gyre) or below (e.g. altimetry). These depth-specific, or depth-relevant, analyses are now
231 possible using satellite data, which combined with knowledge of physical oceanography may allow the sub-
232 surface carbonate system conditions, internal ocean transport and the mixing of water from the interface into
233 the upper ocean to be determined. For example, the evaluation of the impact of near-surface gradients
234 (discussed in section 3.1.1) relies upon the depth specific nature of satellite thermal infrared observations

235 and surface to depth export fluxes have been estimated based on ocean colour satellite observations (Stukel
236 *et al.*, 2023). A thorough understanding of atmosphere-ocean interactions combined with satellite
237 measurements of surface winds has enabled the vertical and horizontal water flow in the Californian
238 upwelling and its influence on the carbonate system to be determined (Quilfen *et al.*, 2021). Similarly, the
239 analysis of altimeter observed eddies analysed alongside *in situ* data and knowledge of their rotation
240 characteristics has allowed the regional significance of eddy-driven vertical mixing to be quantified (Ford *et*
241 *al.*, 2023), which could easily be applied globally.

242

243 Upper ocean turbulence and mixing of all ocean constituents including carbon is predominantly driven by
244 atmospheric winds at the ocean-atmosphere interface. However, there are clear disparities between existing
245 wind re-analysis data products which are critical for quantifying ocean carbon and the observed storm tracks
246 from polar lows and tropical cyclones (e.g., Verezemskaya *et al.*, 2017). The significance of this disparity is
247 likely to grow as the intensity and frequency of storms changes with the changing climate (e.g., Bhatia *et al.*,
248 2019) and these inconsistencies are likely impacting more than just surface turbulence estimates, as storms
249 are known to alter upper ocean mixing and vertical motions which influence temperature, salinity and biology
250 (e.g., Reul *et al.*, 2020) and they can interact with the barrier layer in the upper ocean to inhibit vertical
251 mixing (Balaguru *et al.*, 2012). Different satellite technologies offer a selection of complementary capabilities
252 to address these issues. Satellite scatterometers can provide high spatial resolution observations of low to
253 medium wind speed and direction, but their sensitivity is reduced at higher speeds (e.g., Polverari *et al.*,
254 2021), whereas new advances in polarised synthetic aperture radar have enabled the wind speeds (but not
255 direction) within the eyes of storms to be resolved (e.g., Mouche *et al.*, 2019), although the coverage of the
256 storm within the satellite view can be limited. New passive microwave approaches show high sensitivity to
257 cyclone wind speed and direction, but at relatively low spatial resolutions (e.g., Reul *et al.*, 2017).

258 Intelligently and consistently combining data from all satellite approaches would enable an observation-
259 based wind-speed and direction dataset relevant for all wind conditions with more consistent wind
260 distributions, and work has begun in this area (e.g., the MAXSS project, <https://www.maxss.org/>).

261 Consistency between observation-based wind and wave climate data records will be needed to enable the
262 creation of an upper turbulence climate data record, as extreme waves do not always occur coincident with
263 extreme winds (Hell *et al.*, 2021). These approaches would be suitable for addressing disparities in wind re-
264 analysis data products, leading to a better quantification and understanding of upper ocean turbulence and
265 mixing through time (and would benefit advances in air-sea exchange, by providing consistent wind and
266 wave data for use in gas exchange parameterisations, as discussed in section 3.1.1). Existing satellites
267 networks could enable these advancements, and coverage and understanding will improve further with new
268 proposed satellite wind missions (e.g., Kilic *et al.*, 2018) and proposed active microwave satellite sensors
269 hold the potential to further increase knowledge of surface ocean mixing by directly observing atmosphere
270 and ocean surface velocities and ocean current interactions (e.g., Ardhuin *et al.*, 2019; Gommenginger *et al.*,
271 2019; Morrow *et al.*, 2019).

272

273 **3.1.3 Constraining land to ocean carbon flow**

274 Various methods are used to characterise land to ocean flow of inorganic carbon by rivers including *in situ*
275 upscaling methods (e.g. Regnier *et al.*, 2013), ocean inverse model estimates (Jacobson *et al.*, 2007) and
276 ocean sink estimates (Watson *et al.*, 2020), or atmosphere inversion based approaches (Rödenbeck *et al.*,

277 2018). Despite the plethora of approaches there is lively debate over the river transport value, and its
278 temporal variability, any potential long-term trends, and how these relate to human activity are all poorly
279 constrained (e.g. Regnier *et al.*, 2013b; Lacroix *et al.*, 2020 and Regnier *et al.*, 2022). Hence annual carbon
280 assessments conducted by the global carbon budget rely on long-term static values. Satellite observations
281 are well placed to characterise this flow and an example method presented in Panel 1 suggests that the
282 Amazon inter-annual variation in dissolved inorganic carbon outflow is $\pm 10\%$. Combining high-quality data
283 from existing satellites (e.g., Sentinels 2 and 3) with data from commercial CubeSats (that have higher
284 spatial resolution and observation frequency, but lower spectral quality) and gauging stations could enable
285 satellite observation-based methods to characterise global land-to-ocean flow of carbon for inclusion within
286 global assessments. This characterisation could include its magnitude, variability, any long-term trends and
287 causal factors, the latter of which is likely to change with time. Such combined use of agency and
288 commercial satellite sensors is already used for monitoring global coral health (Li *et al.*, 2019).

289

290 **3.1.4 Towards the study of meso-scale phenomena**

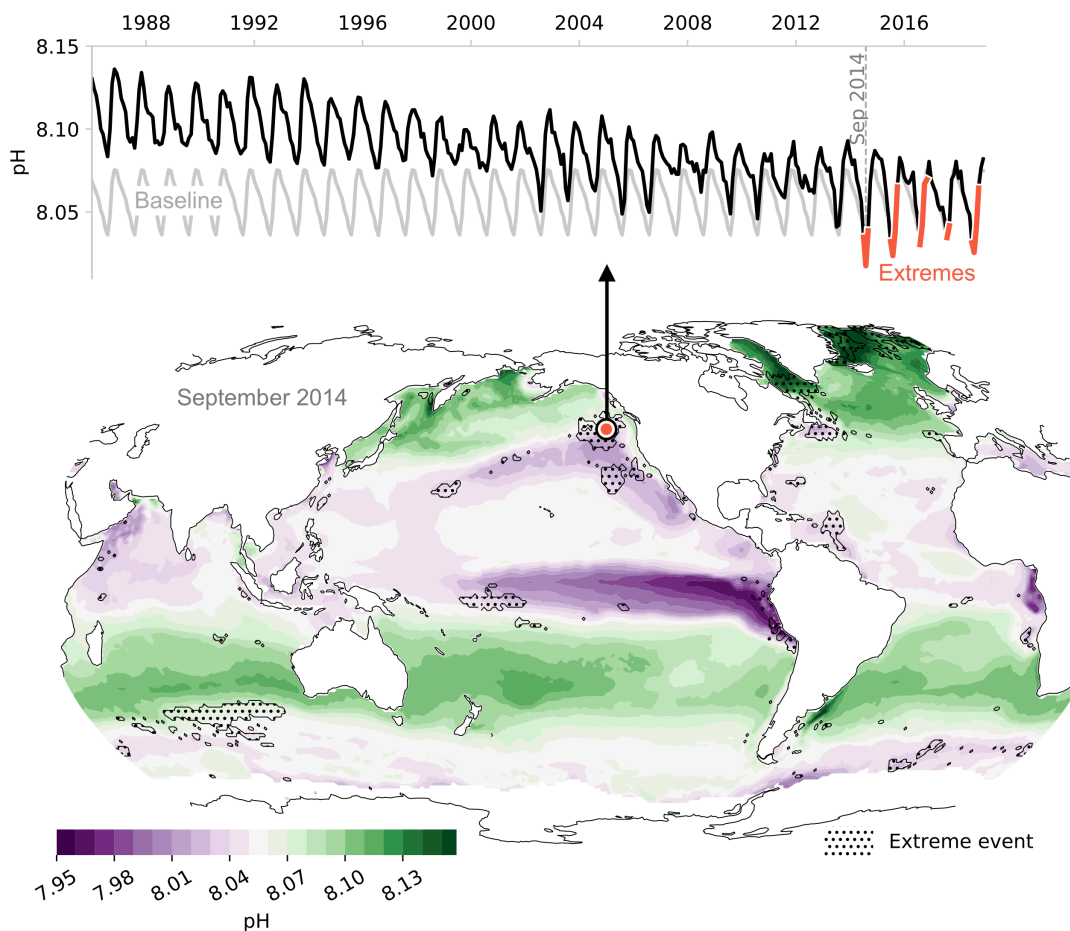
291 Current satellite observation-based datasets for individual carbon system parameters (e.g. alkalinity, Land *et al.*
292 *et al.*, 2019) and the complete marine carbonate system (Gregor and Gruber, 2021) are monthly data at 1°
293 resolution (~ 110 km at the equator). Whilst these demonstrate the potential of such methods and are useful
294 for seasonal-scale or global analyses, they are clearly less useful for regional or local assessments and
295 understanding, particularly when some conditions and interactions can be high frequency or short lived (e.g.,
296 Desmet *et al.*, 2021). These existing methods could be further developed to provide close to weekly and ~ 25
297 km resolutions, as the key underlying observations important for higher-frequency changes in the carbonate
298 system are available at these scales (e.g. temperature at ~ 25 km as the first order controller of the gaseous
299 quantity of CO_2), whilst those observations only available at lower resolutions due to sensing constraints
300 (e.g. salinity at >50 km spatial resolution useful for alkalinity) are characterising aspects that change more
301 slowly. At a basic level using these higher resolution inputs would enable the extension or re-training of
302 existing published algorithms to become near-coastal in regions where a high density of near-coast *in situ*
303 data already exist (e.g., California Current upwelling region). The focus on only deriving higher resolution
304 versions of those parameters needed to isolate the higher-frequency (rather than doing so for all parameters)
305 means that this approach could be applied to global analyses. These higher resolution data are likely to be
306 more useful for regional and local users wishing to identify the extent to which their regional waters are
307 already being impacted by ocean acidification. The increasing amount of globally available higher resolution
308 optical and microwave satellite observations (e.g., daily at <60 m from Sentinel 1, Sentinel 2, Landsat, Planet
309 Labs) mean it is now possible to view or resolve sub-mesoscale features and these could support
310 investigations into any errors within ocean carbon sink assessments (e.g. as studied by Gloege *et al.*, 2021).

311

312 **3.1.5 Identifying regional compound events**

313 Of special concern are the interactions of the changes in ocean chemistry with other concurrent changes,
314 especially warming, but also deoxygenation, pollution, and fishing pressures often termed compound events
315 (e.g. Gruber *et al.*, 2021). These compound events often occur in the aftermath of marine heatwaves (e.g.,
316 Frölicher and Laufkötter, 2020) and tend to add an additional dimension of stress to the already stressed
317 ecosystems (Gruber *et al.*, 2021) which can impact all tropic levels. The ability to use satellite-observation
318 data to derive heat wave duration and extent (e.g., Oliver *et al.*, 2020), surface ocean carbonate data

319 (Gregor and Gruber, 2021) and atmosphere-ocean carbon flux data (e.g. Watson *et al.*, 2020) offers the
320 potential to identify where and when these compound events are occurring (figure 3) and to probe the impact
321 of heat waves on the surface ocean carbon system. Increasing the temporal and spatial resolution of existing
322 datasets (section 3.1.4) and exploiting experimental or operational higher frequency satellite approaches
323 (e.g., Planet Labs dove network, or those mentioned in figure 1a) could enable the detection and analysis of
324 shorter and more intense individual extreme conditions and any resulting compound events. They may also
325 enable precursor events or conditions to be identified as indicators of future change towards short-term
326 forecasting (e.g., 6 monthly). Machine learning (e.g., time-series forecasting) could then likely enable
327 observation (satellite and *in situ*) driven short-term forecasting aligned with the needs of policy makers and
328 marine users (Arico *et al.*, 2021).
329



330

Figure 3: The ability to identify global and regional conditions and variability across all marine carbonate system parameters means that we can now study regional changes in pH to identify where and when ecosystems are experiencing extreme conditions (determined using data from Gregor and Gruber, 2021).

331

332 3.1.6 Identifying and capturing the role of biology

333 Phytoplankton biological growth can modulate surface water CO₂ concentrations as CO₂ in the water is used
334 during photosynthesis, but is also respired, and CO₂ is the net output from calcification (e.g. Ford *et al.*,
335 2022; and as reviewed by Brewin *et al.*, 2021). This biological control, how future changes in biology may
336 alter the oceanic sink of CO₂ and how changes in biological growth can indicate ocean health and stress
337 have all been identified as important areas of research (e.g., Arico *et al.*, 2021). Satellite-observations are

338 already extensively used to study biological carbon (Brewin *et al.*, 2021). But currently the majority of
339 observation-based ocean carbon sink data used within carbon assessments (e.g. within Friedlingstein *et al.*,
340 2021) focus on observations of ocean physics to intelligently interpolate the sparse surface *in situ* gaseous
341 CO₂ data, so these are likely to overlook biological control mechanisms. Climate-quality satellite ocean
342 colour observations (e.g., Sathyendranath *et al.*, 2019) offer the opportunity to include biology within these
343 interpolation schemes. Assessments have been attempted using satellite observed chlorophyll-a estimates
344 (as an indicator of photosynthetic processes) which is a good first step (e.g. Gregor *et al.*, 2021). But
345 evaluations should also focus on satellite-based primary production or net community production data (as
346 reviewed by Brewin *et al.*, 2021) that are more likely to capture the fuller impact of biology on surface water
347 gaseous CO₂ (Ford *et al.*, 2022) and the inclusion of calcification processes that is likely to be important in
348 some regions (Shutler *et al.*, 2013). More work is needed to extend some methods and datasets to achieve
349 global coverage and to build more complete uncertainty budgets (e.g., for net community production). Ocean
350 colour observations, upon which these biological data partly rely, are not retrievable during low light periods,
351 polar winters or below clouds (but biology may still exist), and these data also contain integrated
352 contributions across multiple optical depths within the water and so may not be purely near surface. So
353 methods exploiting these satellite data for surface assessments will need to be able to handle missing or
354 masked data and avoid making assumptions about the underlying biological state when observations are
355 missing, and should consider optical depth. As a first step, a hierarchical approach could be used for regions
356 of missing data, where the method progressively moves through a list of ranked datasets until data coverage
357 is found (e.g., satellite observations, then re-analysis data with the last option being a long-term
358 observational mean). Addressing the issue of missing data is an aspect that should be considered by the
359 satellite observation community to increase the usability of their data, as example machine learning and
360 statistical methods exist (e.g., Liu and Wang, 2022). But these now need to be used within climate data
361 records following the example of the sea surface temperature community who provide gap filled daily data
362 records (Merchant *et al.*, 2019).

363

364 **3.2 Overcoming barriers to the utility and full exploitation of satellite observations**

365 Most remote sensing data and approaches are unlikely to achieve the same precision and accuracy as
366 laboratory measurements, whilst satellite sensor performance can also change over time as the sensor and
367 optics age. Similarly, all field-deployed *in situ* instrumentation, such as buoys or floats, can have instrument
368 performance lower than their laboratory equivalent and their performance can degrade over time (e.g., due
369 to biofouling, calibration drift, damage, or battery degradation). This means that both space-based and *in*
370 *situ* observations have their own unique capabilities, advantages, and individual characteristics to consider.
371 Therefore the evaluation of the utility of satellite observation approaches should focus on what they can they
372 provide that is complementary to other observations or measurements, such as providing higher frequency
373 sampling in space and time (e.g., to enable global assessments, for studying river outflows or episodic
374 events) and sampling where other types of observations are sparse, impractical, or impossible (e.g., polar
375 regions or regions that experience piracy). Then the accuracy and precision of these satellite observations
376 with respect to reference measurements defines how to interpret these data and their potential applicability
377 to a given scientific question. For example, identifying the existence of long-term change or short-lived
378 episodic events versus attempting to precisely identify the rate or range of change of a specific carbonate
379 parameter have very different needs in terms of uncertainties. Consequently, assessing the utility of satellite

380 observations solely by comparing their precision and accuracy to that possible from laboratory analyses is a
381 mistake. Along with the intended application, such assessments should also consider differences in
382 sampling in time and space between different observation techniques (laboratory analyses, *in situ*
383 instrumentation and satellites) as ignoring them can introduce artificial errors (e.g., Land *et al.*, 2023).
384 Overlooking the uncertainties associated with the reference data (e.g., laboratory or *in situ*) being used can
385 also lead to misleading performances (e.g., Ford *et al.*, 2021). Furthermore, for some applications (e.g.,
386 identifying the existence of long-term change and its direction) it will be more important to use temporally
387 stable (long-term) data sources to minimise bias and maximise the precision, rather than concentrating
388 purely on the accuracy of the approach (e.g., using a climate data record; see Taylor, 1967 for an
389 explanation of the underlying statistics). Assessing the utility and potential applications of satellite
390 observations requires consideration of all of these points.

391

392 **3.3 The need for aligned scientific communities**

393 As discussed, it is clear that marine carbon assessments are heavily reliant on satellite observations, and
394 there are a large amount of observations available, each with individual nuances; however, the reasons for
395 specific data choices that are used within these assessments are not always clear. For example, the majority
396 of the satellite observation datasets chosen within data submissions to the global carbon budget
397 (Friedlingstein *et al.*, 2022) focus on operational datasets (e.g. Donlon *et al.*, 2012), designed for short-term
398 forecasting systems, whereas climate-quality data would be more appropriate (e.g. Boutin *et al.*, 2021; Dodet
399 *et al.*, 2021; Merchant *et al.*, 2019; Sathyendranath *et al.*, 2019). These non-optimal dataset choices may be
400 driven by the specific time period being studied, the spatial extent, the visibility of the dataset, uncertainties,
401 a lack of confidence in the data or a misunderstanding of the nuances and intricacies of these satellite
402 observations (e.g. see the extensive content within Robinson 2010) and the potential impact of different
403 choices. Similarly, key studies that are guiding community methods and priorities contain misunderstanding
404 of the use and interpretation of satellite data. For example, Fay, Gregor *et al.*, (2021) misinterpret what
405 satellite chlorophyll-a data represent (referring to them as surface biological activity) potentially leading to
406 incorrect conclusions about their efficacy. Gloege *et al.*, (2021) use satellite observations extensively but
407 omit the data sources or versions, and Gloege *et al.*, (2021) and Lefèvre *et al.*, (2021) overlook the
408 associated data uncertainties (e.g., river plume contamination causing increased chlorophyll-a uncertainties).
409 Irrespective of the reasons for these errors - poor or inconsistent dataset choice and reporting,
410 misunderstandings in capabilities, and overlooking uncertainties are all likely to limit the quality of these
411 carbon assessments and community guidance with implications for policy development.

412

413 Given the high reliance on satellite data for supporting policy, and its potential role in mitigation, adaptation
414 and conservation approaches, the formation of an international expert advisory group to support optimal use
415 of satellite observation datasets and novel sensors or products within carbon assessments and relevant
416 policy is now needed. This would also enable the carbon community to guide the satellite observation
417 community in identifying and providing the most appropriate data for key scientific questions, and enable the
418 exchange of knowledge on uncertainty assessments, data standards and metadata. This would support the
419 goals of the Observing Air-Sea Interactions Strategy (OASIS, Cronin *et al.*, 2022) and the carbon aims and
420 interests of the Committee of Earth Observation Satellites (CEOS) (and more widely the Global Ocean
421 Observing System, GOOS, and Global Climate Observing System, GCOS), and it could also support and

422 guide efforts by the *in situ* communities to develop a network of reference observations (Wanninkhof *et al.*,
423 2019); with mutual benefits as reference observations are needed to assess satellite data-based products.
424 This advisory group would need to consist of multi-sensor satellite and *in situ* experts and could be led by the
425 International Ocean Colour Coordinating Group (IOCCG) or the Group for High Resolution Sea Surface
426 Temperature (GHRST) as both have experience of developing cross-disciplinary groups. These efforts
427 would greatly benefit from support and input from the International Ocean Carbon Coordination project
428 (IOCCP), with key input from climate teams (e.g. the various ESA Climate Change Initiative teams) and
429 individual experts where coordinating groups or climate teams do not exist (e.g. for satellite observed
430 atmospheric column integrated gases). Advances will only be possible through collaboration and co-
431 developed work to guide and identify the advantages of linking expert knowledge across the communities.
432 Collectively, this could lead to aligned communities in terms of data knowledge, availability, visibility,
433 accessibility and standards. This exchange of knowledge could also help support ocean acidification groups
434 by accelerating the integration of different sources of marine carbon data for supporting decision making
435 (e.g., towards holistic representations of current and future ocean acidification conditions and short-term
436 monitoring).

437

438 **3.4 Informing climate adaptation and mitigation measures**

439 Local and regional approaches to minimize the effects of ocean acidification are emerging with a much
440 stronger focus on adaptation and local mitigation (Gattuso *et al.*, 2015). These approaches often work
441 towards effective legislative and governance mechanisms that incorporate ocean acidification data to
442 underpin adaptation and mitigation strategies (Dobson *et al.*, 2022). This includes i) measures to better
443 protect the organisms and ecosystems under stress from ocean acidification against other compound threats
444 (e.g. from overfishing or physical destruction); ii) measures that aim to repair the system (e.g., by building
445 artificial reefs, restoring blue carbon ecosystems or by adding alkaline substances to offset the effect of
446 ocean acidification) and iii) measures to combat the more local or regional drivers of high acidity and low pH
447 conditions, (e.g., by reducing local eutrophication, pollution, and coastal erosion, Kelly *et al.*, 2011).
448 Common to all three approaches is the need for high quality observations, both to assess the level of threat
449 and exposure to the local organisms and ecosystems, as well as to measure the potential success or co-
450 benefit of any action. While *in-situ* based systems are developing and expanding rapidly in some areas of the
451 world, satellite-based observations are now of a sufficient quality to provide a global perspective and
452 constraints for many regions that are only marginally observed. Importantly, satellite observation-based data
453 can be used to call attention to the plight of the oceans in the context of climate change by highlighting
454 regions already under stress and taking on risk (figure 1b; figure 3). There is potential to link satellite
455 observations with the conditions being experienced by some species, the need to support increased
456 understanding of satellite methods within some communities (particularly climate policy leads and marine
457 managers), and the opportunity to co-develop interpretation or indicator methods with key users (Panel 2).
458 The need to increase ocean acidification awareness and literacy more widely has been identified by the UN
459 Decade endorsed Ocean Acidification Research for Sustainability programme OARS (Dobson *et al.*, 2022)
460 and imagery based on satellite observational-based data could support this (e.g., figure 1b). In this way,
461 satellite observation-based data could now be used to aid bottom-up initiatives, to support communities in
462 planning adaptation, management, and monitoring strategies and top-down initiatives to allow policy makers
463 to identify those regions most at risk, highlight their plight and identify necessary mitigation and adaptation

464 needs (Wible, 2021; e.g., figure 3). These same approaches could be applied to support action on, and
465 understanding of, other compounding issues of ocean health (e.g., eutrophication in the coastal zone),
466

467 A satellite and *in situ* based observing system for climate adaption and mitigation that is now possible
468 (Shutler *et al.*, 2020) is needed to support these actions by providing targeted and useful data to a broad
469 user base. To do so, the observing system would need the following characteristics: (i) access to data in
470 marginally observed regions, or regions where little *in situ* data are collected to enable 'new users', (ii) data
471 must be retrieved with high resolution in time and space, especially in regions of concern, (iii) data must be
472 easily and quickly available after their retrieval, and (iv) any ocean carbon data need to be well integrated
473 within other data streams addressing marine stressors, and (v) to ensure uptake and use of these data, it is
474 likely that efforts need to be co-designed with end users (including climate policy leads and marine
475 managers) and undertaken in such a way as to provide suitable data visualization or analysis tools (e.g. Kain
476 and Covi, 2013) and to train early adopters, stakeholders and users in how to use these tools and interpret
477 any data.

478

479 **3.5 Actively demonstrating the value of advances in estimating the ocean carbon sink**

480 The concept of a digital twin component or that of observing system simulation experiment could now be
481 used to illustrate the powerful constraint that ocean carbon sink estimates have on global carbon
482 assessments. This would be a digital representation of the global carbon cycle, with a focus on ocean
483 carbon assessments along with representation of all major sources, pools and sinks of carbon and its
484 redistribution within the Earth system (figure 4). By assuming fossil fuel combustion is well known (box 7;
485 figure 4) this approach can be used to identify closure of the budget, and how improvements in ocean carbon
486 sink estimates impact that closure. All components of this approach are already being routinely used by
487 international groups in a pre-operational, ad-hoc, or distributed manner (e.g., a similar approach is used to
488 assess budget closure within annual assessments, Friedlingstein *et al.*, 2022) so efforts for the
489 implementation would focus purely on addressing technical aspects (e.g., data storage, timely data access,
490 computing requirements, consistency of implementations, full and consistent documentation, testing
491 frameworks etc). Such an approach would allow the importance of the advances made through satellite
492 observation-based methods to be evaluated and highlighted (i.e., the developments identified in section 3.1
493 of this paper). It could also be used to identify where scientific community effort is best focussed to improve
494 assessments, used to assess the scientific and policy advice impact of major national funding decisions to
495 infrastructure, whilst also being used to automate routine assessments to simplify the monitoring of the
496 present state of the ocean to support conservation, mitigation and global carbon assessments; and in doing
497 so, support the aims of sections 3.2, 3.3 and 3.4 of this paper.

498

499 These capabilities could be demonstrated and evaluated under a range of scientific and policy focussed
500 'what if' scenarios including: what happens to the ocean carbon sink estimate and global budget closure if
501 we include ocean eddies, ocean biology, or novel *in situ* data types within the analyses (e.g., Argo floats,
502 gliders, autonomous vessels)? And what happens to the budget closure if the uncertainties within the ocean
503 observational constraint or the river to ocean carbon flow are reduced? Or what happens to the strength of
504 any resultant policy advice if key *in situ* ocean observation networks are funded, versus not funded?
505

506 This approach would help address the needs in the UNESCO and IOC decadal roadmap for ocean carbon
 507 (Arico et al., 2021) by i) highlighting, clarifying, elevating and promoting the use of satellite observations
 508 within ocean carbon analyses and understanding, ii) being used to help evaluate the importance of biology
 509 within ocean carbon assessments, iii) helping identify beneficial approaches for long-term support of the *in*
 510 *situ* ocean carbon observing system and iv) demonstrating how a satellite observation-based system in
 511 conjunction with *in situ* networks, and model re-analyses can be constructed to support policy.
 512

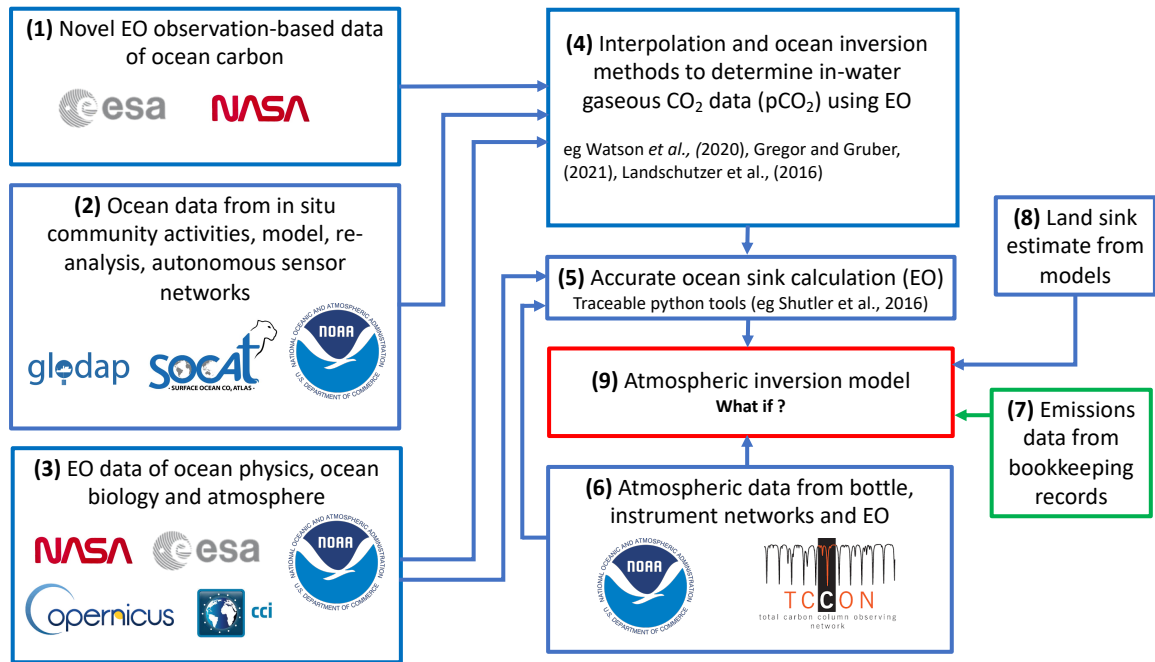


Figure 4: The digital twin component structure of an observing system simulation experiment approach to identify the strength of the observation-based carbon sink estimates. The logos within each module element give typical agency and community data providers. Boxes in blue are where satellite Earth observation data are exploited within global assessments (e.g., Friedlingstein *et al.*, 2022). Techniques typically used for the boxes in green and red are beginning to use satellite observations through new carbon emissions focused satellite missions, and this exploitation is expected to continue increasing.

513

514

515 4.0 Conclusions

516 The urgency of providing the most accurate and precise ocean carbon assessments within the next 5 years,
 517 and to continue refining them is highlighted by the latest IPCC reports where they warn of the need to
 518 drastically reduce carbon emissions. Whilst the performance of any ocean assessments will govern, or limit,
 519 the ability to clearly identify the ocean and carbon budget response to ongoing emissions. Such data will
 520 continue to be needed following any emissions reduction to help track the response of the Earth system.
 521 The heavy reliance and necessity of satellite Earth observation data to enable global ocean carbon
 522 assessments is now scientifically clear and this importance has been recognised by the United Nations
 523 Education Scientific and Cultural Organisation (UNESCO) and the International Oceanographic Commission
 524 (IOC). Combined with the powerful constraint that ocean carbon data have on global carbon assessments,
 525 this importance demonstrates the need to focus efforts on further advancing the use of satellite observations.
 526 The importance of space-based salinity, temperature and wind speed data within assessments and for

527 enabling new scientific capabilities and insight continues to grow, and despite large advances remains
528 relatively under exploited. Alongside this, it is likely that satellite retrieved ocean colour in particular will
529 become increasingly important for these assessments, along with satellite sea-state, ocean currents and
530 atmospheric column integrated gas observations. Greater community cohesion and co-design between
531 satellite, *in situ*, and modelling researchers/users focussing on the carbon system will increase the potential
532 for greater scientific advances, further increase the strength of the ocean constraint within carbon
533 assessments, and enable the advances to actively guide ocean mitigation and conservation efforts. There is
534 a need for sustained effort and funding to provide expert guidance on the use of satellite observations within
535 carbon studies and assessments, to provide support for the key ocean *in situ* measurements that underpin
536 the satellite approaches, and to underpin these efforts within annual carbon assessments used to guide
537 policy, marine management and behavioural change. This policy advice would be considerably strengthened
538 by the formation of an integrated multi-platform observing system with satellite data at the heart; an
539 approach that is now scientifically and physically possible.

540

541 **5.0 Acknowledgements**

542 The authors gratefully acknowledge the support of the European Space Agency grant numbers
543 4000137603/21/I-DT and 4000132954/20/I-NB.

544

545 **6.0 References**

546 Arduin F, Brandt P, Gaultier L, Donlon C, Battaglia A, Boy F, Casal T, Chapron B, Collard F, Cravette S, *et*
547 *al.*, (2019) SKIM, a Candidate Satellite Mission Exploring Global Ocean Currents and Waves. *Frontiers in*
548 *Marine Science*, doi: 10.3389/fmars.2019.00209

549

550 Arico S, Arietta JM, Bakker DCE, Boyd PW, Cotrim da Cunha L, Chai L, Dai F, Gruber N, Isensee K, Ishii N,
551 *et al.*, *Integrated ocean carbon research: a summary of ocean carbon research, and vision of coordinated*
552 *ocean carbon research and observations for the next decade*. UNESCO and the IOC, online, UNESCO,
553 Paris, 45 pages, (2021).

554

555 Balaguru, K., Chang, P., Saravanan, R., Leung, L.R., Xu, Z., Li, M., Hsieh, J.S., (2012) Ocean barrier layers'
556 effect on tropical cyclone intensification. *Proceedings of the National Academy of Sciences*, 109(36),
557 pp.14343-14347

558

559 Bakker, D. C. E., Pfeil, B. Landa, C. S., Metzl, N., O'Brien, K. M., Olsen, A., Smith, K., Cosca, C., Harasawa,
560 S., Jones, S. D., Nakaoka, S., Nojiri, Y., Schuster, U., Steinhoff, T., Sweeney, C., Takahashi, T., Tilbrook, B.,
561 Wada, C., Wanninkhof, R., Alin, S. R., Balestrini, C. F., Barbero, L., Bates, N. R., Bianchi, A. A., Bonou, F.,
562 Boutin, J., Bozec, Y., Burger, E. F., Cai, W.-J., Castle, R. D., Chen, L., Chierici, M., Currie, K., Evans, W.,
563 Featherstone, C., Feely, R. A., Fransson, A., Goyet, C., Greenwood, N., Gregor, L., Hankin, S., Hardman-
564 Mountford, N. J., Harlay, J., Hauck, J., Hoppema, M., Humphreys, M. P., Hunt, C. W., Huss, B., Ibáñez, J.
565 S. P., Johannessen, T., Keeling, R., Kitidis, V., Körtzinger, A., Kozyr, A., Krasakopoulou, E., Kuwata, A.,
566 Landschützer, P., Lauvset, S. K., Lefèvre, N., Lo Monaco, C., Manke, A., Mathis, J. T., Merlivat, L., Millero,
567 F. J., Monteiro, P. M. S., Munro, D. R., Murata, A., Newberger, T., Omar, A. M., Ono, T., Paterson, K.,
568 Pearce, D., Pierrot, D., Robbins, L. L., Saito, S., Salisbury, J., Schlitzer, R., Schneider, B., Schweitzer, R.,

569 Sieger, R., Skjelvan, I., Sullivan, K. F., Sutherland, S. C., Sutton, A. J., Tadokoro, K., Telszewski, M., Tuma,
570 M., Van Heuven, S. M. A. C., Vandemark, D., Ward, B., Watson, A. J., Xu, S. (2016) A multi-decade record
571 of high quality fCO₂ data in version 3 of the Surface Ocean CO₂ Atlas (SOCAT). *Earth System Science Data*,
572 8, 383-413. doi:10.5194/essd-8-383-2016.

573

574 Bakker, D. C.E, De Baar, H. J.W, De Jong, E., (1999) The dependence on temperature and salinity of
575 dissolved inorganic carbon in East Atlantic surface waters, *Marine Chemistry*, 65 (3-4), doi: 10.1016/S0304-
576 4203(99)00017-1

577

578 Bellenger, H., Bopp, L., Ethé, C., Ho, D., Duvel, J.P., Flavoni, S., Guez, L., Kataoka, T., Perrot, X., Parc, L.,
579 Watanabe, M., (2023). Sensitivity of the global ocean carbon sink to the ocean skin in a climate model.
580 *Journal of Geophysical Research: Oceans*, 128(7), p.e2022JC019479.

581

582 Bhatia, K. T., Gabriel A. Vecchi, Thomas R. Knutson , Hiroyuki Murakami, James Kossin, Keith W. Dixon,
583 Carolyn E. Whitlock (2019) Recent increases in tropical cyclone intensification Rates. *Nature*
584 *Communications*, 10:635

585

586 Boutin, J., Reul, N., Koehler, J., Martin, A., Catany, R., Guimbard, S., Rouffi, F., Vergely, J.L., Arias, M.,
587 Chakroun, M., *et al.* (2021) Satellite-Based Sea Surface Salinity Designed for Ocean and Climate Studies.
588 *Journal of Geophysical Research Oceans*, 126, e2021JC017676.

589

590 Brewin RJW, Sathyendranath, S., Kulk, G., *et al.*, (2023) Ocean carbon from space: current status and
591 priorities for the next decade, *Earth-Science Reviews*, doi:1 [0.1016/j.earscirev.2023.104386](https://doi.org/10.1016/j.earscirev.2023.104386)

592

593 Brewin RJW, Sathyendranath S, Platt T, Bouman H, Ciavatta S, Dall'Olmo G, Dingle J, Groom S, Jönsson B,
594 Kostadinov TS, *et al.*, (2021) Sensing the ocean biological carbon pump from space: a review of capabilities,
595 concepts, research gaps and future developments. *Earth-Science Reviews*, 217, 103604-103604

596

597 CEOS (2014) CEOS strategy for carbon observations from space, The Committee on Earth Observation
598 Satellites (CEOS) Response to the Group on Earth Observations (GEO) Carbon Strategy, September 30
599 2014.

600

601 Chau, T. T. T., Gehlen, M., Chevallier, F. (2022) A seamless ensemble-based reconstruction of surface
602 ocean pCO₂ and air–sea CO₂ fluxes over the global coastal and open oceans, *Biogeosciences*, 19, 1087–
603 1109, <https://doi.org/10.5194/bg-19-1087-2022>.

604

605 Ciani *et al.*, (2019) Copernicus Imaging Microwave Radiometer (CIMR) Benefits for the Copernicus Level 4
606 Sea-Surface Salinity Processing Chain, *Remote Sensing*, doi: 10.3390/rs11151818

607

608 Cronin *et al.*, (2022) Developing an Observing Air-Sea Interactions Strategy (OASIS) for the global ocean,
609 *ICES Journal of Marine Science*, doi: 10.1093/icesjms/fsac149

610

611 Desmet, F., Gruber, N., Köhn, E. E., Münnich, M., Vogt, M. (2022) Tracking the Space-Time Evolution of
612 Ocean Acidification Extremes in the California Current System and Northeast Pacific. *Journal of Geophysical*
613 *Research: Oceans*, 127(5), e2021JC018159. Doi: 10.1029/2021JC018159
614
615 Dickson, A.G., Sabine, C.L., Christian, J.R. (2007) Guide to Best Practices for Ocean CO₂ Measurements,
616 *PICES Special Publication 3*, 191 pp.
617
618 Dixon AM, Forster PM, Heron SF, Stoner AMK, Beger M (2022) Future loss of local-scale thermal refugia in
619 coral reef ecosystems. *PLOS Climate* 1(2): doi: 10.1371/journal.pclm.0000004
620
621 Dobson KL, Newton JA, Widdicombe S, Schoo KL, Acquafredda MP, Kitch G, Bantelman A, Lowder K,
622 Valauri-Orton A, Soapi K, Azetsu-Scott K, Isensee K (2022) Ocean Acidification Research for Sustainability:
623 Co-designing global action on local scales. *ICES Journal of Marine Science*, doi:
624 doi.org/10.1093/icesjms/fsac158
625
626 Dodet, G., Piolle, J.-F., Quilfen, Y., Abdalla, S., Accensi, M., Arduin, F., Ash, E., Bidlot, J.-R.,
627 Gommenginger, C., Marechal, G., Passaro, M., Quartly, G., Stopa, J., Timmermans, B., Young, I., Cipollini,
628 P., and Donlon, C. (2020) The Sea State CCI dataset v1: towards a sea state climate data record based on
629 satellite observations, *Earth System Science Data*, 12, 1929–1951, doi: 10.5194/essd-12-1929-2020.
630
631 Doney, Scott C, Busch, D. S., Cooley, S. R., Kroeker, K. J., (2020) The Impacts of Ocean Acidification on
632 Marine Ecosystems and Reliant Human Communities. *Annual Review of Environment and Resources* 45 (1):
633 83–112, doi:10.1146/annurev-environ-012320-083019.
634
635 Donlon, C. J., *et al.*, (2012) The Operational Sea Surface Temperature and Sea Ice Analysis (OSTIA)
636 system, *Remote Sensing of Environment*, 116, pp. 140-158 (DOI: 10.1016/j.rse.2010.10.017).
637
638 Fabry, V. J., Seibel, B. A., Feely, R. A., Orr, J. C. (2019) Impacts of ocean acidification on marine fauna and
639 ecosystem processes. *ICES Journal of Marine Science*, 65, 185–195. Doi: 10.2307/j.ctv8jnz1.25
640
641 Fay, A. R., Gregor, L., Landschützer, P., McKinley, G. A., Gruber, N., Gehlen, M., Iida, Y., Laruelle, G. G.,
642 Rödenbeck, C., Roobaert, A., Zeng, J. (2021) SeaFlux: harmonization of air-sea CO₂ fluxes from surface
643 pCO₂ data products using a standardized approach. *Earth System Science Data*, 13(10), 4693–4710.
644 <https://doi.org/>
645
646 Feely, R A, Doney, S C, Cooley, S. C., (2009) Ocean Acidification: Present Conditions and Future Changes
647 in a High-CO₂ World. *Oceanography* 22 (4): 36–47. doi: 10.5670/oceanog.2009.106.
648
649 Fine R., Willey, D. A, Millero, F. J., (2016) Global variability and changes in ocean total alkalinity from
650 Aquarius satellite data, *Geophysical Research Letters*, doi: 10.1002/2016GL071712
651

652 Friedlingstein *et al.*, (2019) Global Carbon Budget 2019, *Earth System Science Data*, 11, 1783–1838,
653 doi:10.5194/essd-11-1783-2019

654

655 Friedlingstein *et al.*, (2020) Global Carbon Budget 2020, *Earth System Science Data*, 12, 3269–3340, doi:
656 10.5194/essd-12-3269-2020.

657

658 Friedlingstein *et al.*, (2021) Global Carbon Budget 2021, *Earth System Science Data*, doi: 10.5194/essd-14-
659 1917-2022

660

661 Ford D, Tilstone GH, Shutler JD, Kitidis V, Lobanova P, Schwarz J, Poulton AJ, Serret P, Lamont T, Chuqui
662 M, *et al.*, (2021) Wind speed and mesoscale features drive net autotrophy in the South Atlantic Ocean.
663 *Remote Sensing of Environment*, 260, 112435-112435

664

665 Ford, D. J., Tilstone, G. H., Shutler, J. D., Kitidis, V. (2022) Derivation of seawater $p\text{CO}_2$ from net community
666 production identifies the South Atlantic Ocean as a CO_2 source, *Biogeosciences*, 19, 93–115, doi:
667 10.5194/bg-19-93-2022

668

669 Ford DJ, Tilstone GH, Shutler JD, Kitidis V, Sheen KL, Dall’Olmo G, Orselli IBM (2023). Mesoscale Eddies
670 Enhance the Air-Sea CO_2 Sink in the South Atlantic Ocean. *Geophysical Research Letters*, 50(9)

671

672 Gentemann *et al.*, (2019) FluxSat: Measuring the Ocean–Atmosphere Turbulent Exchange of Heat and
673 Moisture from Space, *Remote Sensing*, doi: 10.3390/rs12111796

674

675 Gloege, L., McKinley, G. A., Landschützer, P., Fay, A. R., Frölicher, T. L., Fyfe, J. C., *et al.* (2021).
676 Quantifying Errors in Observationally Based Estimates of Ocean Carbon Sink Variability. *Global*
677 *Biogeochemical Cycles*, 35(4), e2020GB006788

678

679 Goddijn-Murphy, L. M., Woolf, D. K., Land, P. E., Shutler, J. D., and Donlon, C. (2015) The OceanFlux
680 Greenhouse Gases methodology for deriving a sea surface climatology of CO_2 fugacity in support of air–sea
681 gas flux studies, *Ocean Science*, 11, 519–541, doi: 10.5194/os-11-519-2015

682

683 Gommenginger *et al.*, (2019) SEASTAR: A Mission to Study Ocean Submesoscale Dynamics and Small-
684 Scale Atmosphere-Ocean Processes in Coastal, Shelf and Polar Seas, *Frontiers in Marine Science*, doi:
685 10.3389/fmars.2019.00457

686

687 GOA-ON (2019) GOA-ON (Global Ocean Acidification Observing Network), 2019. “Global Ocean
688 Acidification Observing Network (GOA-ON) Implementation Strategy, 2019.” [http://www.goa-](http://www.goa-on.org/documents/general/GOA-ON_Implementation_Strategy.pdf)
689 [on.org/documents/general/GOA-ON_Implementation_Strategy.pdf](http://www.goa-on.org/documents/general/GOA-ON_Implementation_Strategy.pdf)

690

691 Green, H., Findlay, H., Shutler, J. D., Land, P. E., Bellerby, R. G. J., (2021), Satellite Observations Are
692 Needed to Understand Ocean Acidification and Multi-Stressor Impacts on Fish Stocks in a Changing Arctic
693 Ocean, *Frontiers in Marine Science*, 8, p692, <https://doi.org/10.3389/fmars.2021.635797>

694

695 Gregor, L., Gruber, N. (2021) OceanSODA-ETHZ: a global gridded data set of the surface ocean carbonate
696 system for seasonal to decadal studies of ocean acidification, *Earth System Science Data*, 13, 777–808,
697 <https://doi.org/10.5194/essd-13-777-202>

698

699 Gruber, N., Landschützer, P., Lovenduski, N. S. (2019) The variable southern ocean carbon sink, *Annual*
700 *Review of Marine Science*, 2019 11:1, 159-186

701

702 Gruber, N., Clement, D., Carter, B. R., Feely, R. A., van Heuven, S., Hoppema, M., *et al.* (2019b). The
703 oceanic sink for anthropogenic CO₂ from 1994 to 2007. *Science*, 363(6432), 1193–1199.
704 <https://doi.org/10.1126/science.aau5153>

705

706 Gruber, N., Boyd, P.W., Frölicher, T.L. *et al.* (2021) Biogeochemical extremes and compound events in the
707 ocean. *Nature* 600, 395–407. doi: 10.1038/s41586-021-03981-7

708

709 Gruber, N., Bakker, D. C. E. , DeVries, T., Gregor, L., Hauck, J., Landschützer, P., McKinley, G. A., Müller, J.
710 D., (2023) Trends and variability of the ocean carbon sink, *Nature Reviews Earth and Environment*, 4, pages
711 119–134

712

713 Gattuso, J.- P., Magnan, A., Bille, R., Cheung, W. W. L., Howes, E. L. , Joos, F., Allemand, D., *et al.* (2015)
714 Contrasting Futures for Ocean and Society from Different Anthropogenic CO₂ Emissions Scenarios. *Science*
715 349 (6243): aac4722–aac4722, doi:10.1126/science.aac4722.

716

717 Hell, M.C., Ayet, A., Chapron, B., (2021) Swell generation under extra-tropical storms. *Journal of*
718 *Geophysical Research: Oceans*, 126(9), p.e2021JC017637.

719

720 Ho, D., *et al.*, (2006) Measurements of air-sea gas exchange at high wind speeds in the Southern Ocean:
721 Implications for global parameterizations, *Geophysical Research Letters*, doi: 10.1029/2006GL026817

722

723 Jacobson, A. R., Fletcher, S. E. M., Gruber, N., Sarmiento, J. L., Gloor, M. (2007) A joint atmosphere-ocean
724 inversion for surface fluxes of carbon dioxide: 1. Methods and global-scale fluxes. *Global Biogeochemical*
725 *Cycles*, doi:10.1029/2005gb002556

726

727 Keeling (1978) Atmospheric carbon dioxide in the 19th century, *Science*, doi:
728 10.1126/science.202.4372.1109

729

730 Kain, D., Covi, M (2013) Visualizing complexity and uncertainty about climate change and sea level rise,
731 *Communication Design Quarterly*, doi: 10.1145/2466489.2466499

732

733 Keil, K. E., Feifel, K. M., Russell, N. B., (2021) Understanding and Advancing Natural Resource
734 Management in the Context of Changing Ocean Conditions, *Coastal Management*, 49:5, 458-486, doi:
735 10.1080/08920753.2021.1947127

736
737 Kelly, R P, M M Foley, W S Fisher, R A Feely, B S Halpern, G G Waldbusser, M R Caldwell (2011) Mitigating
738 Local Causes of Ocean Acidification with Existing Laws. *Science* 332 (6033): 1036–37.
739 <https://doi.org/10.1126/science.1203815>.

740 Kilic, L., Prigent, C., Aires, F., Boutin, J., Heygster, G., Tonboe, R. T., Roquet, H., Jimenez, C., Donlon, C.
741 (2018), Expected performances of the Copernicus Imaging Microwave Radiometer (CIMR) for an all-weather
742 and high spatial resolution estimation of ocean and sea ice parameters. *Journal of Geophysical Research:*
743 *Oceans*, 123, doi: 10.1029/2018JC014408

744 Lacroix, F., Ilyina, T., & Hartmann, J. (2020) Oceanic CO₂ outgassing and biological production hotspots
745 induced by pre-industrial river loads of nutrients and carbon in a global modeling approach. *Biogeosciences*,
746 17(1), 55–88. <https://doi.org/10.5194/bg-17-55-2020>
747

748 Land P.E., Shutler J.D., Findlay H., Girard-Ardhuin F., Sabia R., Reul N., Piolle J., Chapron B., Quilfen Y.,
749 Salisbury J.E., *et al* (2015) Salinity from space unlocks satellite-based assessment of ocean acidification,
750 *Environmental Science & Technology*, 49 (4), pp 1987–1994, doi: 10.1021/es504849s
751

752 Land P.E., Findlay H.S., Shutler J.D., Ashton I.G., Holding T., Grouazel A., Girard-Ardhuin F., Reul N., Piolle
753 J.F., Chapron B., Quilfen Y., (2019) Optimum satellite remote sensing of the marine carbonate system using
754 empirical algorithms in the global ocean, the Greater Caribbean, the Amazon Plume and the Bay of
755 Bengal, *Remote Sensing of Environment*, 235, p.111469, doi: 10.1016/j.rse.2019.111469
756

757 Lauvset, S. K., Lange, N., Tanhua, T., Bittig, H. C., Olsen, A., Kozyr, A., Álvarez, M., Becker, S., Brown, P.
758 J., Carter, B. R., Cotrim da Cunha, L., Feely, R. A., van Heuven, S., Hoppema, M., Ishii, M., Jeansson, E.,
759 Jutterström, S., Jones, S. D., Karlsen, M. K., Lo Monaco, C., Michaelis, P., Murata, A., Pérez, F. F., Pfeil, B.,
760 Schirnack, C., Steinfeldt, R., Suzuki, T., Tilbrook, B., Velo, A., Wanninkhof, R., Woosley, R. J., and Key, R. M.
761 (2021) An updated version of the global interior ocean biogeochemical data product, GLODAPv2.2021, *Earth*
762 *System Science Data*, 13, 5565–5589, doi:10.5194/essd-13-5565-2021,
763

764 Lee, K., Tong, L. T., Millero, F. J., Sabine, C. L., Dickson, A. G., Goyet, C., Park, G. -H. , Wanninkhof, R.
765 Feely, R. A., Key, R. M. (2006), Global relationships of total alkalinity with salinity and temperature in surface
766 waters of the world's ocean. *Geophysical Research Letter.*, 33, L19605,
767

768 Lefèvre N., Mejia, C., Khvorostyanov D., Beaumont, L., Koffi U., (2021) Ocean Circulation Drives the
769 Variability of the Carbon System in the Eastern Tropical Atlantic. *Oceans*, 2(1), 126-148
770

771 Li *et al.*, (2019) Object-Based Mapping of Coral Reef Habitats Using Planet Dove Satellites *Remote Sensing*,
772 11, doi: 10.3390/rs11121445
773

774 Liu, X., Wang, M., (2022) Global daily gap-free ocean color products from multi-satellite measurements,
775 *International Journal of applied Earth observation and geoinformation*, 108, 102714, doi
776 :[10.1016/j.jag.2022.102714](https://doi.org/10.1016/j.jag.2022.102714)
777

778 Merchant, C.J., Embury, O., Bulgin, C.E. *et al.* (2019) Satellite-based time-series of sea-surface temperature
779 since 1981 for climate applications. *Scientific Data* **6**, 223. <https://doi.org/10.1038/s41597-019-0236-x>
780

781 Millero, F. J., Lee, L., Roche, M. P. (1998), Distribution of alkalinity in the surface waters of the major
782 oceans, *Marine Chemistry*, 60, 111– 130.
783

784 Minnett *et al.*, (2019) Half a century of satellite remote sensing of sea-surface temperature, *Remote Sensing*
785 *of Environment*, doi: 10.1016/j.rse.2019.111366
786

787 Morrow, R., Fu, L-L., Arduin, F., Benkiran, M., Chapron, B., Cosme, E., d'Ovidio, F., Farrar, J.T., Gille, S.T.,
788 Lapeyre, G., Le Traon, P-Y., Pascual, A., Ponte, A., Qiu, B., Rasclé, N., Ubelmann, C., Wang, J., and Zaron,
789 E.D. (2019), Global Observations of Fine-Scale Ocean Surface Topography with the Surface Water and
790 Ocean Topography (SWOT) Mission, *Frontiers in Marine Science*, 6, doi: 10.3389/fmars.2019.00232
791

792 Mouche, A., B. Chapron, J. Knaff, Y. Zhao, B. Zhang, and C. Combot, (2019) Copolarized and cross-
793 polarized SAR measurements for high-resolution description of major hurricane wind structures: Application
794 to Irma category 5 hurricane, *Journal of Geophysical Research*, 124, 3905-3922.
795

796 Nagel, L., Krall, K. E., and Jähne, B.: Comparative heat and gas exchange measurements in the Heidelberg
797 Aeolotron, a large annular wind-wave tank, *Ocean Science*, 11, 111–120, [https://doi.org/10.5194/os-11-111-](https://doi.org/10.5194/os-11-111-2015)
798 2015, 2015
799

800 Land, P. E., Findlay, H. S., Shutler, J. D., Piolle, J.-F., Sims, R., Green, H., Kitidis, V., Polukhin, A., and
801 Pipko, I. I., (2023) OceanSODA-MDB: a standardised surface ocean carbonate system dataset for model–
802 data intercomparisons, *Earth System Science Data*, 15, 921–947, doi: 10.5194/essd-15-921-2023.
803

804 Oliver, E. C. J. J., Benthuyssen, J. A., Darmaraki, S., Donat, M. G., Hobday, A. J., Holbrook, N. J., Schlegel,
805 R. W., Gupta, A. Sen, & Sen Gupta, A. (2021) Marine Heatwaves. *Annual Review of Marine Science*, 13(1),
806 1–30. Doi: 10.1146/annurev-marine-032720-095144
807

808 Olivier, L., Boutin, J., Reverdin, G., Lefèvre, N., Landschützer, P., Speich, S., Karstensen, J., Labaste, M.,
809 Noisel, C., Ritschel, M. *et al.* (2022) Wintertime process study of the North Brazil Current rings reveals the
810 region as a larger sink for CO₂ than expected. *Biogeosciences*, 19, 2969-2988, doi:10.5194/bg-19-2969-
811 2022.
812

813 Orr JC, Fabry VJ, Aumont O, *et al.*, (2005) Anthropogenic ocean acidification over the twenty-first century
814 and its impact on calcifying organisms. *Nature*, 437: 681– 86
815

816 Phillips *et al.*, (2006) Maximum entropy modelling of species geographic distributions, *Ecological Modelling*,
817 190, doi: 10.1016/j.ecolmodel.2005.03.026

818

819 Polverari, F., Portabellow, M., Lin, W., *et al.* (2021) On High and Extreme Wind Calibration Using ASCAT,
820 *IEEE Transactions on Geoscience and Remote Sensing*, doi:10.1109/TGRS.2021.3079898

821

822 Quilfen Y, Shutler J, Piolle J-F, Autret E (2021) Recent trends in the wind-driven California current upwelling
823 system, *Remote Sensing of Environment*, 261, 112486-112486.

824

825 Reul, N., B. Chapron, E. Zabolotskikh, C. Donlon, A. Mouche, J. Tenerelli, F. Collard, J.F. Piolle, A. Fore, S.
826 Yueh, J. Cotton, P. Francis, Y. Quilfen, and V. Kudryavtsev, (2017) A new generation of tropical cyclone size
827 measurements from space. *Bulletin of the American Meteorology Society*, 98, 2367-2385,
828 doi:10.1175/BAMS-D-15-00291.1

829

830 Reul, N., Chapron, B., Grodsky, S.A., Guimbar, S., Kudryavtsev, V., Foltz, G.R. and Balaguru, K., (2021)
831 Satellite observations of the sea surface salinity response to tropical cyclones. *Geophysical Research*
832 *Letters*, 48(1), p.e2020GL091478

833

834 Robinson (2010) *Discovering the ocean from space, the unique applications of satellite oceanography*,
835 Springer, ISBN: 978-3-540-68322-3

836

837 Rödenbeck, C., Zaehle, S., Keeling, R., Heimann, M. (2018) How does the terrestrial carbon exchange
838 respond to inter-annual climatic variations? A quantification based on atmospheric CO₂ data,
839 *Biogeosciences*, 15, 2481-2498.

840

841 Regnier, P., Friedlingstein, P., Ciais, P., Mackenzie, F. T., Gruber, N., Janssens, I. a., *et al.* (2013)
842 Anthropogenic perturbation of the carbon fluxes from land to ocean. *Nature Geoscience*, 6(8), 597–607.
843 <https://doi.org/10.1038/ngeo1830>

844 Regnier, P., Friedlingstein, P., Ciais, P., Mackenzie, F. T., Gruber, N., Janssens, I. a., *et al.* (2013b)
845 Anthropogenic perturbation of the carbon fluxes from land to ocean. *Nature Geoscience*, 6(8), 597–607.
846 <https://doi.org/10.1038/ngeo1830>

847 Regnier, P. A. G., Resplandy, L., Najjar, R. G., Ciais, P. (2022). The land-to-ocean loops of the global carbon
848 cycle. *Nature*, 2022 603:7901, 603(7901), 401–410. doi: 10.1038/s41586-021-04339-9

849

850 Sabine *et al.*, (2004) The oceanic sink for anthropogenic CO₂, *Science*, doi: 10.1126/science.109740

851

852 Salisbury, J., Vandemark, D., Jönsson, B., Balch, W., Chakraborty, S., Lohrenz, S., *et al.* (2015) How can
853 present and future satellite missions support scientific studies that address ocean acidification?
854 *Oceanography* 28, 108–121. doi: 10.5670/oceanog.2015.35

855

856 Sathyendranath, S, Brewin, RJW, Brockmann, C, Brotas, V, Calton, B, Chuprin, A, Cipollini, P, Couto, AB,
857 Dingle, J, Doerffer, R, Donlon, C, Dowell, M, Farman, A, Grant, M, Groom, S, Horseman, A, Jackson, T,
858 Krasemann, H, Lavender, S, Martinez-Vicente, V, Mazeran, C, Mélin, F, Moore, TS, Müller, D, Regner, P,
859 Roy, S, Steele, CJ, Steinmetz, F, Swinton, J, Taberner, M, Thompson, A, Valente, A, Zühlke, M, Brando, VE,
860 Feng, H, Feldman, G, Franz, BA, Frouin, R, Gould, Jr., RW, Hooker, SB, Kahru, M, Kratzer, S, Mitchell, BG,
861 Muller-Karger, F, Sosik, HM, Voss, KJ, Werdell, J, and Platt, T (2019) An ocean-colour time series for use in
862 climate studies: the experience of the Ocean-Colour Climate Change Initiative (OC-CCI). *Sensors*, 19, 4285.
863 doi:10.3390/s19194285

864

865 Shutler J.D., Land P.E., Brown C.W., Findlay H.S., Donlon C.J., Medland M., Snooke R., Blackford J.C.,
866 (2013) Coccolithophore surface distributions in the North Atlantic and their modulation of the air-sea flux of
867 CO₂ from 10 years of satellite Earth observation data. *Biogeosciences*, 10(4), 2699-2709.

868

869 Shutler J.D., Quartly G.D., Donlon C.J., Sathyendranath S., Platt T., Chapron B., Johannessen J.A., Girard-
870 Arduin F., Nightingale P.D., Woolf D.K., *et al.*, (2016) Progress in satellite remote sensing for studying
871 physical processes at the ocean surface and its borders with the atmosphere and sea-ice. *Progress in*
872 *Physical Geography*, 40, 215-246.

873

874 Shutler J.D., Wanninkhof R., Nightingale P.D., Woolf D.K., Bakker D.C., Watson A., Ashton I.G., Holding T.,
875 Chapron B., Quilfen Y., Fairall C., (2020). Satellites will address critical science priorities for quantifying
876 ocean carbon, *Frontiers in Ecology and the Environment*, doi: 10.1002/fee.2129

877

878 Sunday, J., Fabricius, K., Kroeker, K. *et al.*, (2017) Ocean acidification can mediate biodiversity shifts by
879 changing biogenic habitat. *Nature Climate Change*, 7, 81–85. <https://doi.org/10.1038/nclimate3161>

880

881 Stukel, M.R., Irving, J.P., Kelly, T.B. *et al.* (2023) Carbon sequestration by multiple biological pump pathways
882 in a coastal upwelling biome. *Nature Communications*, 14. doi: 10.1038/s41467-023-37771-8

883

884 Takahashi *et al.*, (1997) Global air-sea flux of CO₂: An estimate based on measurements of air-sea pCO₂
885 difference, *Proceedings of the National Academy of Sciences*, doi: 10.1073/pnas.94.16.829

886

887 Taylor, J. R., (1976) An introduction to error analysis, the study of uncertainties in physical measurements,
888 Second edition, University Science Books, ISBN-13: 978-0-935702-75-0

889

890 Tilbrook B, Jewett EB, DeGrandpre MD, Hernandez-Ayon JM, Feely RA, Gledhill DK, Hansson L, Isensee K,
891 Kurz ML, Newton JA, Siedlecki SA, Chai F, Dupont S, Graco M, Calvo E, Greeley D, Kapsenberg L, Lebrech
892 M, Pelejero C, Schoo KL and Telszewski M (2019) An Enhanced Ocean Acidification Observing Network:
893 From People to Technology to Data Synthesis and Information Exchange. *Frontiers in Marine Science*,
894 6:337. doi: 10.3389/fmars.2019.00337

895

896 Verezhemskaya, P., Tilinina, N., Gulev, S., Renfrew, I. A., Lazzara, M. (2017). Southern Ocean mesocyclones
897 and polar lows from manually tracked satellite mosaics. *Geophysical Research Letters*, 44(15), 7985–7993.

898

899 Wanninkhof, R., Pickers, P.A., Omar, A.M., Sutton, A., Murata, A., Olsen, A., Stephens, B.B., Tilbrook, B.,
900 Munro, D., Pierrot, D., Rehder, G., (2019) A surface ocean CO₂ reference network, SOCONET and
901 associated marine boundary layer CO₂ measurements. *Frontiers in Marine Science*, 6, p.400.

902

903 Watson, A.J., Schuster, U., Shutler, J.D. *et al.*, (2020) Revised estimates of ocean-atmosphere CO₂ flux are
904 consistent with ocean carbon inventory. *Nature Communications*. 11, 4422.

905

906 Wibble, B., (2021), Out of harms way, *Science*, 372, 6548, pp. 1274-1275, doi: 10.1126/science.abi9209.

907

908 Woolf D.K., Land P.E., Shutler J.D., Goddijn-Murphy L.M., Donlon C.J., (2016) On the calculation of air-sea
909 fluxes of CO₂ in the presence of temperature and salinity gradients. *Journal of Geophysical Research:*
910 *Oceans*, 121(2), 1229-1248.

911

912 Woolf DK, Shutler JD, Goddijn - Murphy L, Watson AJ, Chapron B, Nightingale PD, Donlon CJ, Piskozub J,
913 Yelland MJ, Ashton I, *et al* (2019). Key Uncertainties in the Recent Air - Sea Flux of CO₂. *Global*
914 *Biogeochemical Cycles*, 33(12), 1548-1563.

915

916 Widdicombe, S., Isensee, K., Artioli, Y., Gaitán-Espitia, J.D., Hauri, C., Newton, J.A. , Wells, M., Dupont, S.,
917 (2023) Unifying biological field observations to detect and compare ocean acidification impacts across
918 marine species and ecosystems: What to monitor and why, *Ocean Sciences*, doi: 10.5194/os-19-101-2023

919

920 7.0 Appendix

921

922 The following sections detail the methods for the example land to ocean carbon flow estimate.

923

924 7.1 Integrated carbon mass across the depth of the Amazon river plume

925 Ocean surface total dissolved inorganic carbon (CT) concentration data were obtained for the period 2010 to
926 2020 from a publically available monthly gridded CT time series (Sims *et al.*, 2022). This dataset
927 encompasses the whole Amazon outflow region including regions that mainly contain oceanic water masses
928 from the South Atlantic, so it is necessary to first distinguish between the oceanic waters and those relating
929 to the river plume. The Amazon river plume was identified using sea surface salinity (SSS) specified as any
930 grid cells with SSS < 35 (as used by Coles *et al.*, 2013; Hu *et al.*, 2004). The monthly gridded time series
931 data are a surface dataset and so do not include subsurface values through the total plume depth, so plume
932 depth is needed to quantify the total riverine CT. To account for changes in SSS and likely CT concentration
933 with depth, the mean SSS throughout the plume, S_{plume} , was calculated from surface SSS using the
934 relationship described by Hu *et al.*, (2004):

935

$$936 S_{plume} = 4.352 + SSS * 0.881 \quad (1)$$

937

938 The depth integrated CT concentration of each plume grid cell (CT_{plume}) was then calculated using S_{plume} and
939 by assuming CT is conservative with salinity using:

940

$$941 CT_{plume} = CT_{surf} \frac{S_{plume}}{SSS} \quad (2)$$

942

943 where CT_{surf} is the monthly mean surface CT concentration. Total plume CT (CT_{total}) for a given month can
944 then be calculated by summing CT_{plume} for each grid cell within the plume (as identified by regions SSS <
945 35). In an effort to separate out the riverine CT from the oceanic originating CT, the proportion of CT in each
946 plume grid cell which originates from the river, κ , was estimated by assuming conservative mixing with ocean
947 water, and linearly interpolating between 0 and 35 (such that a salinity of 0 indicates 100% riverine source,
948 and 35 indicates 100% oceanic source). The gridded riverine CT ($CT_{riverine}$) is then calculated as:

949

$$950 CT_{riverine} = \kappa CT_{plume} \quad (3)$$

951

952 where κ is the mixing factor. The total carbon mass resulting from $CT_{riverine}$ is then calculated for each grid
953 cell by multiplying $CT_{riverine}$ by plume volume and molecular mass of carbon, m_c , to give:

954

$$955 M_{CT} = V_{plume} CT_{riverine} m_c \quad (4)$$

956

957 where V_{plume} is the volume of the plume for the respective grid cell, calculated by multiplying the grid cell
958 surface area by S_{plume} . Collectively equations 1 to 4 enable a spatial dataset of carbon mass integrated
959 across the depth of the plume to be calculated.

960

961 7.2 Quantifying Amazon river discharge

962 Calculating the flux of carbon originating from the river requires a measure of river flow and the need to
 963 identify a region or location across which the river plume flow is measured or quantified. Along a river this
 964 measurement location would be a river gauging station where the flow is channelled, but here the data give
 965 the plume as it extends into the ocean. So to quantify the CT discharge as it flows into the ocean a family of
 966 24 radii transects were drawn across the plume, centred on the mouth of the Amazon (figure A1). For each
 967 portion of each radii that intersects with the plume M_{CT} was summed and the monthly riverine CT flow
 968 estimate for each radii transect (i.e. the resultant sum of carbon passing through, or intersecting, each
 969 individual radii) was calculated by dividing the sum of M_{CT} by the monthly Amazon river discharge:
 970

971
$$CT_{outflow,r} = \frac{\sum^{i \in G} M_{CT,i}}{Q} \quad (5)$$

972
 973 where G is the set of all plume grid cells intersecting with the radii transect with radius r, $M_{CT,i}$ is the mass of
 974 CT in grid cell i, and Q is the monthly volume of water discharged by the Obidos gauging station. This
 975 calculation is repeated for all radii and months, producing 24 different estimates of $CT_{outflow}$. Note, that
 976 outflow estimates of zero (i.e. where $G = \emptyset$) were excluded, since this indicated that no plume cells were
 977 intersected by the radii perimeter. This could occur, for example, if there is a break in the plume, or if the
 978 plume does not extend as far as the radii.
 979

980 Choosing an optimal radii is not straightforward, since small radii are more likely to include near-coastal data
 981 where uncertainties in the CT data are likely greater (eg due to land-sea adjacency effects for the satellite
 982 Earth observation inputs), while larger radii will increase the time lag in the calculation because it will
 983 intersect water that is temporally older. This time lag is not expected to always follow a linear relationship
 984 with distance due to temporal and/or spatial variation in plume direction, discharge rate, wind speed and
 985 ocean current interactions. Larger radii, which have larger time lags, are likely to result in larger uncertainties
 986 in the calculations, as the water will have likely experienced more interactions (mixing, chemical alteration or
 987 losses due to gas exchange), and so the grid cells selected by larger radii are less likely to solely contain
 988 water of a similar age.
 989

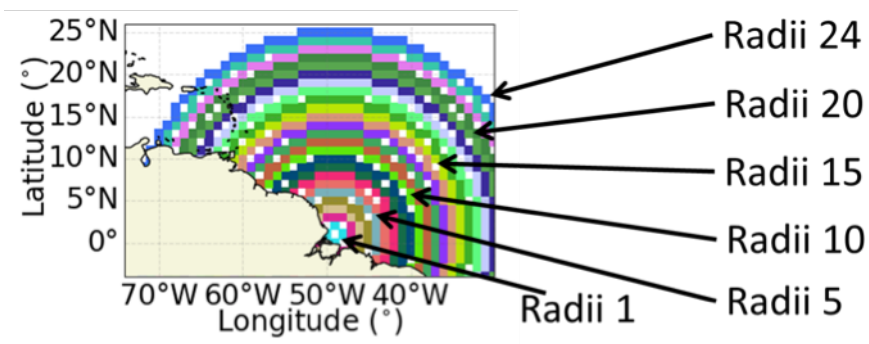


Figure A1 Radii centred on the mouth of the Amazon that were used to quantify the flow of carbon originating from the river plume.

990

991

992 Using the mean CT outflow calculated from multiple radii will reduce the uncertainty associated with coastal
993 cell inaccuracies and variations in plume shape. Conversely, including larger radii increases the time-lag
994 between the mean of river flow variations and the mean identified CT outflow. To mitigate this, CT outflow is
995 calculated from a set of radii, $R = \{1, 2, \dots, n_r\}$, where n_r is chosen to minimise this time-lag. This is done by
996 selecting the n_r that maximises the correlation coefficient between mean seasonal CT outflow and mean
997 seasonal river discharge. The aim is to maximise the number of radii used to estimate the mean, while
998 keeping the size of radii small enough to ensure that the temporal lag is inconsequential at the monthly
999 temporal resolution used. It is expected that this maximum correlation method will be robust to variation in
1000 the calculated mean seasonal (monthly) CT outflow, but it does not always guarantee alignment to the peak
1001 value. For the Amazon dataset the radii 5 gave the highest correlation between the mean seasonal CT
1002 outflow and mean seasonal discharge ($r=0.99$).

1003

1004

1005 **7.3 Uncertainty analysis**

1006 Uncertainties were propagated at each step of equations 1 to 5 and an analysis was conducted to identify
1007 the main sources of uncertainty in CT. The resulting uncertainty in CT outflow combines uncertainties from
1008 the surface CT gridded time series data, discharge data, plume depth relationship (Coles *et al.*, 2013) and
1009 the mean plume salinity (Hu *et al.*, 2004). Standard analytical error propagation methods were used where
1010 possible (see Taylor, 1997). The uncertainty in monthly discharge was estimated as the standard deviation
1011 of the mean monthly discharge (ie assuming that sub-monthly measurements were independent repeated
1012 samples of the monthly mean). Uncertainties in the plume depth were estimated from the 95% confidence
1013 limits shown in figure 13 of Coles *et al.*, (2013). No uncertainties are reported for the relationship between
1014 mean plume salinity and surface salinity in Hu *et al.*, (2004), (which is equation 1) so an estimate of $\pm 10\%$
1015 uncertainty in the coefficients has been used for both intercept and slope.

1016

1017 An analytical approach was not appropriate for determining the uncertainty in the plume mask from SSS
1018 (and therefore plume surface area), and so an ensemble approach was used instead. For this, a set of 100
1019 ensembles were calculated using the SSS dataset with added noise (i.e. sampling 100 times from a grid of
1020 normally distributed random numbers) with a mean equal to the original SSS data set value and standard
1021 deviation equal to the uncertainty in that value for each grid cell:

1022

$$1023 \quad S_{ensemble,i,j} = N(S_{mean,j}, S_{uncertainty,j}) \quad (6)$$

1024

1025 where $S_{ensemble,i,j}$ is the ensemble SSS for the sample i at grid cell j , and $S_{mean,j}$ and $S_{uncertainty,j}$ are the mean
1026 and uncertainty from the SSS data set for grid cell j . The plume masks for each ensemble SSS were
1027 calculated by applying the $SSS < 35$ threshold, leading to an ensemble of 100 separate plume masks.

1028

1029 Uncertainties arising from SSS, including from the plume mask, were propagated using these 100 ensemble
1030 data sets. The calculation was repeated for each ensemble SSS at each stage (equations 1 to 5). This
1031 results in 100 ensemble outputs for each step in the calculation, from which the standard deviation was
1032 calculated to estimate uncertainty at that stage. For example, to calculate uncertainty in the plume surface
1033 area, the surface area of each ensemble plume mask was calculated, and the standard deviation of these

1034 100 surface areas calculated. Similarly, to calculate the uncertainty in mean plume salinity (equation 1)
 1035 arising from the SSS input data, equation 1 was applied to each ensemble, resulting in 100 S_{plume} values
 1036 from which the standard deviation was calculated. In calculating the uncertainty of the CT content of the
 1037 plume (CT_{plume} , from equation 2) the full ensemble of 100 ensemble S_{plume} data sets were used in conjunction
 1038 with the 100 SSS ensembles to propagate this uncertainty forward. Note that the uncertainty propagated
 1039 from SSS data is combined with any other source of uncertainty at each step (e.g. the $\pm 10\%$ on the Hu *et al.*,
 1040 (2004) relationship) resulting in a combined uncertainty estimate for all input data and models, from which
 1041 the standard deviation is calculated to estimate the combined uncertainty of the complete approach.

1042

1043 7.4 Results

1044 The mean annual CT outflow of the Amazon was calculated as $43.7 \pm 3.0 \text{ Tg C yr}^{-1}$ (table 4) with a standard
 1045 deviation of 4.3 Tg C yr^{-1} and a coefficient of variation of 0.10. Therefore the Amazon to Atlantic flow of
 1046 inorganic carbon is estimated to be 44 Tg C yr^{-1} with an annual variation of $\sim 10\%$. Current estimates of land
 1047 to ocean carbon flow are 0.45, 0.60 and 0.78 GtC yr^{-1} (Jacobson *et al.*, 2007; Watson *et al.*, 2020;
 1048 Resplandy *et al.*, 2018; Sarmiento & Sundquist, 1992) and there is much debate over which value to use,
 1049 hence the latest global carbon assessment used the mean value of 0.61 GtC yr^{-1} (Friedlingstein *et al.*, 2020).
 1050 Therefore using 0.61 GtC yr^{-1} as the reference suggests that the Amazon could be responsible for $\sim 7\%$ of
 1051 global land to ocean flow of inorganic carbon and the first estimate of the inter-annual variation in this
 1052 Amazon land to ocean flow is $\pm 10\%$.

1053

Annual results	Mean \pm uncertainty
Amazon discharge	$5.56 \times 10^{12} \pm 5.15 \times 10^8 \text{ m}^3$
Plume surface area	$1.38 \times 10^{12} \pm 3.42 \times 10^9 \text{ m}^2$
Plume thickness	13.2 m
Plume volume	$1.87 \times 10^{13} \pm 7.18 \times 10^{10} \text{ m}^3$
Plume CT	$3.64 \times 10^{13} \pm 4.39 \times 10^{11} \text{ g C}$
CT outflow ($r_n = 5$)	$43.71 \pm 3.00 \text{ Tg C}$

1054 **Table A1:** Annual mean results and standard deviations for each component of the CT outflow calculation
 1055 for the Amazon river based on $r_n = 5$.

1056

1057 References

1058 Coles, V. J., Brooks, M. T., Hopkins, J., Stukel, M. R., Yager, P. L., Hood, R. R. (2013) The pathways and
 1059 properties of the Amazon River Plume in the tropical North Atlantic Ocean, *Journal of Geophysical Research*
 1060 *Ocean*, 118(12), 6894–6913, doi:10.1002/2013JC008981.

1061 Druffel, E. R. M., Bauer, J. E., Griffin, S. (2005) Input of particulate organic and dissolved inorganic carbon
 1062 from the Amazon to the Atlantic Ocean, *Geochemistry, Geophysics, Geosystems*, 6(3),
 1063 doi:10.1029/2004GC000842.

1064 Friedlingstein, P. *et al.*, (2020) Global Carbon Budget 2020, *Earth Syst. Sci. Data*, 12, 3269–3340,
 1065 <https://doi.org/10.5194/essd-12-3269-2020>

1066 Hu, C., Montgomery, E. T., Schmitt, R. W., Muller-Karger, F. E. (2004) The dispersal of the Amazon and
1067 Orinoco River water in the tropical Atlantic and Caribbean Sea: Observation from space and S-PALACE
1068 floats, *Deep Sea Research Part II Tropical Studies in Oceanography*, 51(10-11 SPEC. ISS.), 1151–1171,
1069 doi:10.1016/j.dsr2.2004.04.001.

1070 Jacobson, A. R., Fletcher, S. E. M., Gruber, N., Sarmiento, J. L., Gloor, M. (2007) A joint atmosphere-ocean
1071 inversion for surface fluxes of carbon dioxide: 1. Methods and global-scale fluxes, *Global Biogeochemical*
1072 *Cycles*, 21(1), doi:10.1029/2005GB002556.

1073 Richey, J. E., Hedges, J. I., Devol, A. H., Quay, P. D., Victoria, R., Martinelli, L., Forsberg, B. R. (1990)
1074 Biogeochemistry of carbon in the Amazon River, *Limnology and Oceanography*, 35(2), 352–371,
1075 doi:10.4319/lo.1990.35.2.0352.

1076 Sarmiento, J. L., Sundquist, E. T. (1992) Revised budget for the oceanic uptake of anthropogenic carbon
1077 dioxide, *Nature*, 356(6370), 589–593, doi:10.1038/356589a0.

1078 Sims, R. P., Holding, T. M., Land, P. E., Piolle, J.-F., Green, H. L., Shutler, J. D. (2022) OceanSODA-
1079 UNEXE: A multi-year gridded Amazon and Congo River outflow surface ocean carbonate system dataset,
1080 *Earth System Science Data Discussions*, doi: 10.5194/essd-2022-294

1081 Taylor, J. R. (1997) An introduction to error analysis : the study of uncertainties in physical measurements,
1082 *University Science Books*.

1083 Resplandy, L., Keeling, R. F., Rödenbeck, C., Stephens, B. B., Khatiwala, S., Rodgers, K. B., Long, M. C.,
1084 Bopp, L., Tans, P. P. (2018) Revision of global carbon fluxes based on a reassessment of oceanic and
1085 riverine carbon transport, *Nature Geoscience*, 11, 504–509, <https://doi.org/10.1038/s41561-018-0151-3>.

1086 Watson, A. J., Schuster, U., Shutler, J. D., Holding, T., Ashton, I. G. C., Landschützer, P., Woolf, D. K., and
1087 Goddijn-Murphy, L. (2020) Revised estimates of ocean-atmosphere CO₂ flux are consistent with ocean
1088 carbon inventory, *Nature Communicaions*, 11, 1–6, <https://doi.org/10.1038/s41467-020-18203-3>.

1089
1090
1091
1092
1093
1094

Panel 1: The potential for quantifying land to ocean flow of inorganic carbon

Quantifying extent, magnitude and variability

Land to ocean flow of inorganic carbon by rivers is included within the annual carbon assessments, with an equivalent annual size of 20% to 35% of the contemporary oceanic carbon sink (range taken from Friedlingstein *et al.*, 2022). However, the complexity of these systems, their distribution throughout the world combined with their high heterogeneity means that current assessments assume static values. Given the size of this carbon exchange, improving our ability to monitor them and characterise their flows would help improve closure of the global carbon assessments.

Combining satellite, *in situ* and empirical approaches and data sources

Surface extent and monthly variability of large river flows can be viewed and accurately quantified using satellite data (Land *et al.*, 2019; Sims *et al.*, 2022; Figure P1). These satellite data provide spatially resolved observations, but are limited in their temporal resolution and they are unable to determine the plume depth. Combining empirical understanding from *in situ* analyses with river gauging information and satellite data can enable the depth, flow and spatial extent to be characterised.

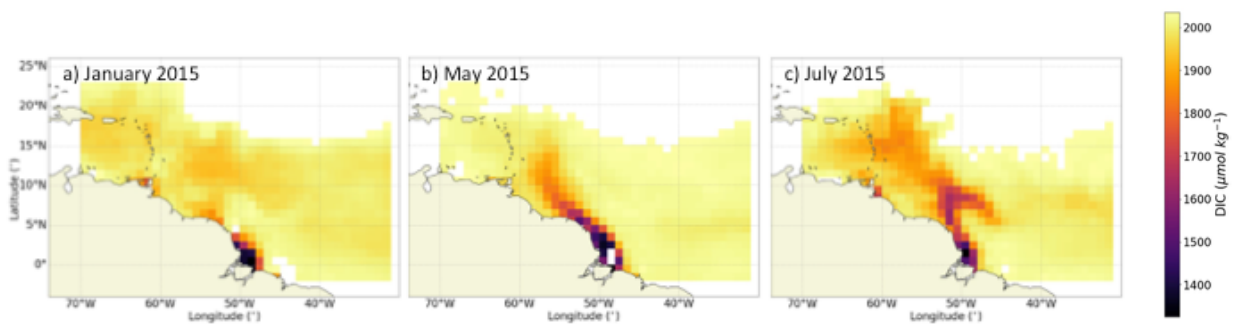


Figure P1: Satellite observation-based estimates of the surface dissolved inorganic carbon within the Amazon plume during three different months in 2015 showing high spatial and temporal variability

Example method

Ocean surface total dissolved inorganic carbon concentration data were obtained from a publicly available Amazon region monthly gridded time series (Sims *et al.*, 2022) and regions where salinity <35 was used to identify the river plume (as used by Hu *et al.*, 2004). The mean salinity and carbon within the plume were calculated from the surface salinity using the relationship described by Hu *et al.*, (2004), from which the depth integrated carbon concentration was calculated, assuming the carbon is conservative with salinity. The riverine carbon estimate was further refined by assuming conservative mixing with ocean water through linearly interpolating between salinity of 0 and 35 (i.e. 0 is 100% riverine, 35 is 100% oceanic). River flow gauging data then allows the carbon flow through an arc that bisects the plume (e.g. equivalent to an offshore gauging station) to be calculated giving a total riverine land to ocean carbon flow with respect to time. Please see the appendix of this paper for the full methods.

This analysis identifies a net flow of 44 terra grams of carbon per year (Tg C yr^{-1}) for the Amazon with an inter-annual variation of $\pm 10\%$. This total flow is equivalent to $\sim 7\%$ of the total annual global riverine flux currently used in global assessments (e.g. as used in Friedlingstein *et al.*, 2021).

Linking satellite observations with species

Space observations will be key for understanding the impact of acidification on economically important marine resources to identify the baseline conditions and variability, and to map life histories of key species against changing conditions (as proposed by Green *et al.*, 2021) towards underpinning management decisions, and where and when to focus remedial efforts. This could be applied to any marine species, but potential foci could be key sentinel species of ecosystem health (e.g., tuna, marine turtles or birdlife), economically, or socially, important fisheries, such as oysters, or artisanal fish species and key plankton species that form the base of the food chain (e.g., pteropods). This could identify regions of interest such as those that are already experiencing high variability in marine carbon conditions, indicate when conditions cross experimentally-derived thresholds of tolerance for particular species, guide where efforts should be focussed to support communities and marine life, or identify highly-variable but healthy ecosystems towards identifying populations with phenotypes more resistant to change. It may be possible to use satellite observations in conjunction with niche modelling approaches (e.g., Phillips *et al.*, 2006) to understand how the existing conditions are impacting the different life stages of each species. And matching satellite observations of carbon, with key biological processes or indicator data could provide quantitative evaluation of the impacts of acidification through time at an ecosystem level (e.g., Widdicombe *et al.*, 2023)

The co-development of indicators and easy access alongside other observations

Many user groups are unlikely to require a deep understanding of the ocean conditions and instead will require the data to be translated into simple indicators. For example, to identify regions that are under-stress, particularly vulnerable, hot spots of activity, or pre-cursor indicators of a potential detrimental change in conditions. To be of most use, ocean acidification data and its complete metadata needs to be assessed in the context of other stressors, especially that of ocean warming, but also coastal eutrophication, coastal habitat destruction and pollution (Gruber *et al.*, 2011). The co-development of these simple indicators, using satellite observation-based data and constructed in ways that are understandable for non-experts, could be used to identify regions or societies that require protection, remedial action or support. For most users, local to regional monitoring information that is available in a timely and easily-accessible manner will be of most relevance, although for major stakeholders (e.g. governments or international assessments) global information is likely to be crucial (e.g., the Inter-governmental Panel on Climate Change, IPCC).

Supporting community understanding and uptake of satellite observations

Training in data interpretation and capacity building are likely to be the main limitations on uptake of satellite-derived information, along with making data easily available to those without reliable internet connectivity. Potential user groups, including policy makers (e.g., country-wide or regional politicians), to regional resource managers (e.g., who determine regional monitoring), to end users (e.g., shellfish growers), will have different needs and understanding. Direct engagement with marine and coastal resource managers who are uniquely working on improving ocean acidification and hypoxia management responses, interventions, and resilience building strategies is essential. For addressing climate change, successful coastal and marine management depends upon an improved understanding of regional ocean and coastal

change and enhanced communication between resource managers and other stakeholder groups (Keil *et al.*, 2021).